

1 **Climate elasticity of streamflow revisited – an elasticity index based on long-**
2 **term hydrometeorological records**

3

4 Vazken Andréassian⁽¹⁾, Laurent Coron^(1,2), Julien Lerat⁽³⁾, Nicolas Le Moine⁽⁴⁾

5 ⁽¹⁾ Irstea, Hydrosystems and Bioprocesses Research Unit (HBAN), Antony, France

6 ⁽²⁾ now at EDF-DTG, Toulouse, France

7 ⁽³⁾ Bureau of Meteorology, Canberra, Australia

8 ⁽⁴⁾ UPMC, Paris, France

9

10 **Abstract**

11 We present a new method to derive the empirical (i.e., data-based) elasticity of
12 streamflow to precipitation and potential evaporation. This method, which uses long-
13 term hydrometeorological records, is tested on a set of 519 French catchments.

14 We compare a total of five different ways to compute elasticity: the reference method
15 first proposed by Sankarasubramanian et al. (2001) and four alternatives differing in
16 the type of regression model chosen (OLS or GLS, univariate or bivariate). We show
17 that the bivariate GLS and OLS regressions provide the most robust solution,
18 because they account for the co-variation of precipitation and potential evaporation
19 anomalies. We also compare empirical elasticity estimates with theoretical estimates
20 derived analytically from the Turc-Mezentsev formula.

21 Empirical elasticity offers a powerful means to test the extrapolation capacity of those
22 hydrological models that are to be used to predict the impact of climatic changes.

23

24 **1. Introduction**

25 **1.1 About hydrological elasticity**

26 In a context of growing uncertainty on water resources due to climate change, simple
27 tools able to provide robust estimates of this impact are essential to support policy
28 and planning decisions. Streamflow elasticity is one such tool: it describes the
29 sensitivity of the changes in streamflow related to changes in a climate variable
30 (Schaake and Liu, 1989). $\varepsilon_{Q/X}$, the elasticity of streamflow Q to a climate variable X
31 is defined by the following equation:

$$\Delta Q / \bar{Q} = \varepsilon_{Q/X} \Delta X / \bar{X} \quad \text{Eq. 1}$$

32 where \bar{Q} and \bar{X} are the long-term average value of streamflow and the climatic
 33 variable, respectively, and the operator Δ indicates the difference between the dated
 34 and the average value. $\varepsilon_{Q/X}$ is nondimensional [% / %], because it is a ratio between
 35 two relative (and thus already nondimensional) quantities. One can also define
 36 elasticity as the ratio between two absolute quantities and, provided both quantities
 37 are expressed in the same unit (for example, mm.yr^{-1} for streamflow, precipitation or
 38 potential evaporation), it would still be a nondimensional ratio [$\text{mm.yr}^{-1} / \text{mm.yr}^{-1}$]. We
 39 will name this absolute elasticity $e_{Q/X}$, defined as:

$$\Delta Q = e_{Q/X} \Delta X \quad \text{Eq. 2}$$

40 Table 1 summarizes the notations used in this paper.
 41

42 1.2 Past studies on elasticity in hydrology

43 ▪ Theoretical (model-based) studies

44 Most of the studies on elasticity are *theoretical*, in the sense that they are based on
 45 flows simulated by a hydrological model fed with different inputs. There are many
 46 examples of such theoretical studies. Nemec and Schaake (1982) used the
 47 Sacramento model, Vogel et al. (1999) used the linear regression coefficients of
 48 annual streamflow models, Sankarasubramanian et al. (2001) used the abcd model,
 49 Niemann and Eltahir (2005) used a purpose-built model and Chiew (2006) used the
 50 SIMHYD and AWBM models. The most widely used model in elasticity studies is the
 51 long-term water balance formula first proposed by Turc & Mezentsev (Mezentsev,
 52 1955; Turc, 1954) (see section 3.2). This formula (sometimes improperly confused
 53 with Budyko's formula) was used in elasticity studies by Dooge (1992), Arora (2002),
 54 Sankarasubramanian et al. (2001), Yang et al. (2008), Potter and Zhang (2009),
 55 Yang and Yang (2011), Donohue et al. (2011) and Yang et al. (2014), among others.
 56

57 ▪ Empirical (data-based) studies

58 Only a few of the published elasticity studies are *empirical*. By *empirical*, we mean
 59 that they use measured data (for different sub-periods) to evaluate the climate
 60 elasticity of streamflow. To our knowledge, Sankarasubramanian et al. (2001) were

61 the first to publish a method based on the median of annual flow anomalies to
62 compute elasticity, later used by Chiew (2006). Potter et al. (2010) analyzed
63 concomitant reductions of precipitation and streamflow in the Murray-Darling basin
64 over three major historic droughts, and Potter et al. (2011) suggested computing
65 elasticity as a multiple linear regression linking annual transformed streamflow values
66 to annual precipitation and temperature anomalies.

67

68 ▪ **Difference between theoretical (model-based) and empirical (data-based)
69 elasticity assessments**

70 To clarify the differences existing between theoretical and empirical elasticity
71 computing approaches, we have listed the key characteristics of both methods in
72 Table 2. The most important problem stems from the co-variation of potential
73 evaporation (or temperature) and precipitation: Fu et al. (2007a) mentioned this issue
74 and proposed to transform the “single parameter precipitation elasticity of streamflow
75 index” into a “two parameter climate elasticity index” which would be function of both
76 precipitation and temperature, in order to account for both effects simultaneously.
77 Recently, Chiew et al. (2013) underline that “because of the inverse correlation
78 between rainfall and temperature, any effect from the residual temperature on
79 streamflow is much less apparent than the direct effect of (the much more variable)
80 rainfall.” Note that the use of model simulations to compute streamflow elasticity
81 circumvents this problem.

82 However, there remains what we consider to be a major disadvantage: since all
83 hydrological models are a simplification of reality, using them to predict changes
84 requires some type of initial validation on empirical (observed) data. Indeed, we have
85 recently compared (see Fig. 9a in Coron et al., 2014) the ability of three models of
86 increasing complexity to reproduce the variations in water balance equilibrium over
87 10-year-long periods and shown that all three models tested had a tendency to
88 underestimate observed changes.

89 In this paper, we will focus on identifying the most robust approach to compute
90 empirical elasticity. Then we will compare the results obtained by this method with
91 the theoretical elasticity of the Turc-Mezentsev water balance formula. This
92 comparison will only aim at illustrating the difference between the two approaches,
93 since there is no reason to consider one or the other as the “true” reference.

94

95 **1.3 Scope of the paper**

96 In this paper, we test four alternative approaches to compute the empirical
97 streamflow elasticity, which we compare over a large catchment set to the approach
98 first suggested by Sankarasubramanian et al. (2001). In section 2, we present the
99 data set of 519 French catchments on which this study is based. Section 3 gives a
100 short overview on the possible graphical representations of catchment elasticity and
101 the methods used to quantify empirical elasticity. Section 4 presents a preliminary
102 selection of the formulas, focusing on the distinction between univariate and bivariate
103 methods. Then section 5 presents a regional analysis of streamflow elasticity to
104 precipitation and potential evaporation over France. Last, the conclusion identifies a
105 few perspectives for further work.

106

107 **2. Catchment dataset**

108 Figure 1 presents the 519 catchments analyzed for these studies.
109 Long series of continuous daily streamflow and precipitation were available over the
110 1976–2006 period. The data set encompasses a variety of climatic conditions
111 (oceanic, Mediterranean, continental, mountainous). Precipitation data was provided
112 by Météo France as a gridded product, based on a countrywide interpolation of rain
113 gage data (SAFRAN product). As far as potential evaporation data is concerned, we
114 used the Penman-Shuttleworth equation (Shuttleworth, 1993). Note that tests
115 implemented with the classical Penman-Monteith *reference evapotranspiration*
116 equation showed little difference (they can be found in the discussion version of this
117 paper), but we preferred to switch to the Penman-Suttlleworth *potential*
118 evapotranspiration formula because Donohue et al. (2010) suggested that it was the
119 most appropriate form of *atmospheric evaporation demand* when considering a
120 changing climate.

121 To illustrate the issues raised this paper, we will use the catchment of the River
122 Brèze at Meyrueis. This 36-km² catchment located in the south of France has a good
123 quality stream-gaging station and a long observation series.

124

125 **3. A review of methods to assess streamflow elasticity**

126 **3.1 Graphical assessment of elasticity**

127 Nemec and Schaake (1982) introduced the classical sensitivity plots showing the
128 changes in streamflow (or in some streamflow-based characteristics) as a function of
129 percent change in precipitation (Figure 2). Their approach consisted in assessing
130 streamflow elasticity over the whole modeling period by gradually changing the
131 model inputs individually. If the hydrological model behavior is free from thresholds or
132 strong hysteresis effects, this method produces a set of parallel curves such as those
133 shown in Figure 2.

134 Wolock and McCabe (1999) used a similar graph (Figure 3), but replaced the percent
135 changes with the absolute changes (plotting $e_{Q/X}$ instead of $\varepsilon_{Q/X}$): in this paper, we
136 will follow their example, but replace the model-based results with observations.

137 The graphs used herein describe *empirical elasticity*: they are based on hydrological
138 data only and require a sub-sampling of long-term records, i.e., distinguishing a
139 number of sub-periods. Therefore, a point is apparent for each of these sub-periods.
140 Figure 4 presents an example in which ΔQ is plotted as a function of either ΔP or
141 ΔE_P .

142 To represent the co-variations of ΔQ with both ΔP or ΔE_P simultaneously, we need
143 either a three-dimensional graph or a graph based on isolines (see Fu et al., 2007b).
144 Figure 4 c presents an example using a color code. This graph is particularly useful
145 because the values of ΔP and ΔE_P are often correlated (Chiew et al., 2013), which
146 may make the two-dimensional representations misleading.

147 The graphical representation of empirical elasticity shown in Figure 4 allows looking
148 at data without formulating an arbitrary modeling choice. The only convention lies in
149 the duration of the sub-periods. Here, we chose a duration of 10 years in order to
150 obtain contrasted yet representative periods. Figure 5 illustrates the changes induced
151 by a change in this duration. It is reassuring to see that similar trends are observed
152 for a wide range of period lengths. The relationship between the different variables
153 does not remain absolutely identical, however, and there is clearly a trade-off
154 between a longer duration, which ensures that the relationships are close to their
155 long-term value, and a lower number of points, which reduces the confidence in the
156 trend displayed by the plot.

157

158 **3.2 Reference method for theoretical elasticity assessment: the Turc-**
159 **Mezentsev formula**

160 Most of previous studies used a model-based definition of elasticity, and several of
161 them used the Turc-Mezentsev formula (Mezentsev, 1955; Turc, 1954). The
162 interested reader can refer to *Lebecherel et al.* (2013) for an historical review on this
163 formula, which is given by:

$$Q = \Psi(P, E_p) = P - \frac{P}{\left(1 + \left(\frac{P}{E_p}\right)^n\right)^{\frac{1}{n}}} = P - \left(P^{-n} + E_p^{-n}\right)^{-\frac{1}{n}} \quad \text{Eq. 3}$$

164 with Q – long-term mean average flow (mm/yr), P – long-term mean average
165 precipitation (mm/yr), E_p – long-term mean average potential evaporation (mm/yr). n
166 is the only free parameter of the formula. Here, we followed *Le Moine et al.* (2007)
167 and used a fixed value $n=2.5$.

168 Partial derivatives of the Turc-Mezentsev formula are easily computed, they are
169 given in Eq. 4 and Eq. 5. They allow computing the theoretical value of the
170 precipitation and potential evaporation elasticity directly for each catchment.

171

$$\frac{\partial Q}{\partial E_p} = \Psi'_p(P, E_p) = -\left(1 + \left(\frac{E_p}{P}\right)^n\right)^{-\frac{n+1}{n}} \quad \text{Eq. 4}$$

$$\frac{\partial Q}{\partial P} = \Psi'_{E_p}(P, E_p) = 1 - \left(1 + \left(\frac{P}{E_p}\right)^n\right)^{-\frac{n+1}{n}} \quad \text{Eq. 5}$$

172

173 **3.3 Alternative methods for empirical streamflow elasticity assessment**

174 We will now focus on data-based methods assessing empirical elasticity. Long-term
175 series of streamflow and catchment climate are required. Before introducing the
176 methods compared in this paper, let us introduce the notation $\Delta X_i^{(M)} = X_i^{(M)} - X^{(LT)}$
177 denoting the departure (anomaly) of a variable X computed over a period of M years
178 starting from year i versus the long-term average $X^{(LT)}$ computed over the entire
179 period.

180

181 Five methods will be compared in this paper, all listed in Table 3.

182

183 • **Nonparametric method**

184 This method computes an annual time-series of relative streamflow anomalies (i.e.,
185 differences with the long-term mean) and then uses the median of these values as an
186 elasticity estimator:

$$\begin{cases} e^{(M)}_{Q/P} = \text{median}\left(\frac{\Delta Q_i^{(M)}}{\Delta P_i^{(M)}}\right) \\ e^{(M)}_{Q/E_p} = \text{median}\left(\frac{\Delta Q_i^{(M)}}{\Delta E_{P_i}^{(M)}}\right) \end{cases} \quad \text{Eq. 6}$$

187 This method is similar to the one advocated by *Sankarasubramanian et al.* (2001)
188 except that they used it to compute the relative rather than the absolute elasticity
189 (see Table 1). In addition, *Sankarasubramanian et al.* (2001) applied the method to
190 yearly data only, whereas we used sub-periods ranging from 1 to 25 years in this
191 study.

192

193 • **Regression methods quantifying precipitation and potential evaporation
194 elasticities (OLS or GLS estimates) independently**

195 These methods compute elasticity as either an ordinary least-square (OLS) or
196 generalized least-square (GLS) solution (Johnston, 1972) of the regression models
197 detailed in Table 4. See Appendix 1 for a quick description of the method used to
198 perform the GLS regression.

199

200 • **Methods quantifying precipitation and potential evaporation elasticities
201 (OLS or GLS estimates) simultaneously**

202 These methods (OLS or GLS) quantify precipitation and potential evaporation
203 elasticities *simultaneously* by looking for the GLS solution of a regression model with
204 the same statistical assumptions as above (see Table 5).

205 The strength of the bivariate method obviously lies in the fact that it accounts for the
206 cross-correlation of ΔP and ΔE_p values. The method used for inferring the parameter
207 values and their significance was identical to the method described above.

208 Note that for the sake of consistency with the GLS models, the uncertainty in the
209 OLS parameters was assessed with the bootstrap approach (Efron and Tibshirani,
210 1994).

211

212 **4. Selection of the best method to compute empirical streamflow
213 elasticity**

214 **4.1 Assessing the capacity of the five methods to compute the empirical
215 elasticity of a synthetic data set**

216 As a first step to compare the merits of the different regression models presented in
217 the previous section, the elasticity estimation was conducted with synthetic
218 streamflow data generated from the Turc-Mezentsev formula, where the parameter n
219 was set at 2.5 (Le Moine et al., 2007). The advantage of using synthetic flow here is
220 that we know the exact (i.e., analytical) solution for elasticity, and this will help
221 identify the drawbacks of some of the methods compared.

222 For this test, the observed streamflow anomalies $\Delta Q_i^{(M)}$ were replaced by the
223 estimates $\tilde{\Delta Q}_i^{(M)} = \Psi(P_i^{(M)}, E_{P_i}^{(M)}) - \Psi(P_i^{(LT)}, E_{P_i}^{(LT)})$ where Ψ is given in Equation 3. The
224 empirical elasticity values were subsequently compared with the exact values
225 $\Psi'_P(P_i^{(LT)}, E_{P_i}^{(LT)})$ and $\Psi'_{E_p}(P_i^{(LT)}, E_{P_i}^{(LT)})$ given in Equations 4 and 5, respectively. The
226 performance of each regression model was judged according to the absolute bias B
227 and root mean square error (RMSE) R :

$$B_X^{(M)} = \left| \sum_{i=1}^N [e_{Q_i/X_i}^{(M)} - \Psi'_x(P_i^{(LT)}, E_{P_i}^{(LT)})] \right| \quad \text{Eq. 7}$$

$$R_X^{(M)} = \sqrt{\sum_{i=1}^N [e_{Q_i/X_i}^{(M)} - \Psi'_x(P_i^{(LT)}, E_{P_i}^{(LT)})]^2} \quad \text{Eq. 8}$$

228 where X is the climate variable (P or E_P), $e_{Q_i/X_i}^{(M)}$ is the corresponding empirical
229 elasticity value computed for catchment i using sub-periods of M years, and $N=519$ is
230 the number of catchments.

231 The performance of the five alternative methods is presented in Figure 6, which
232 shows the absolute bias and the root mean square error on the elasticity for
233 precipitation and potential evaporation, respectively.

234 The four plots in Figure 6 clearly indicate the superiority of the two bivariate models
235 (OLS-2 and GLS-2) over the three univariate models (NP, OLS-1 and GLS-1), with
236 bias and RMSE on both types of elasticity that are lower by several orders of
237 magnitude. This first result suggests that the estimation of empirical elasticity is
238 greatly improved when conducted simultaneously on rainfall and potential
239 evaporation.

240 Figure 6 also shows that the duration of the sub-periods can slightly affect the
241 performance of the regression model. The largest impact can be seen in the bias on
242 the elasticity to potential evaporation (Figure 6.a) where the optimal duration of 20
243 years provides a better performance compared to the other durations. The 20-year
244 duration seems to be the best choice for both types of elasticity, for all regression
245 models, and both bias and RMSE. The only noticeable exception is the bias on
246 elasticity to rainfall (Figure 6.b) for the GLS-2 model where the best elasticity values
247 are obtained for sub-periods of 10 years. This could indicate that the optimal duration
248 may not be identical for the estimation of elasticity to rainfall and potential
249 evaporation.

250

251 This study based on synthetic data shows the clear superiority of the methods based
252 on bivariate regressions (OLS2 and GLS2): the Non-Parametric method (NP) and the
253 univariate regressions (OLS1 and GLS1) are clearly unable to compute streamflow
254 elasticity robustly. Because the NP method is the reference method (suggested by
255 (Sankarasubramanian et al., 2001)), Figure 7(a,c) compares the empirical elasticity
256 values given by the NP method and the GLS2 method: the differences are very large.
257 On the other hand, Figure 7(b,d) shows that there is little difference between the
258 estimates given by OLS2 and GLS2. However, for statistical reasons (presented in
259 Appendix 2) we consider that the GLS solution should probably be preferred.

260 Having decided on the best method to compute empirical elasticity, we can now
261 compare model elasticities with the GLS estimates based on measured streamflow.

262

263 **4.2 Coherence of data-based and model-based elasticity estimates**

264 We now wish to compare the *empirical* elasticity computed with the GLS2 method
265 (the recommended one) with the *theoretical* elasticity derived analytically from the
266 Turc-Mezentsev formula (see Eq. 3). While in the previous test we used synthetic

267 data, we now use the actual (measured) streamflow. This means that contrary to the
268 preceding test, we do not have any “reference”: since neither the data-based nor the
269 model-based elasticity can be considered “true,” we can only assess the coherence
270 between the two computations.

271 The scatterplots illustrated in Figure 8 compare the elasticity values obtained by the
272 multivariate regression (GLS2) method and the model-based approach: we can see
273 that the link between the two measurements on a catchment-by-catchment basis
274 prpis extremely weak for precipitation... and even more for potential evaporation.

275 The fact that empirical and theoretical elasticities differ is in itself noteworthy and
276 would require further analysis. At this point, we cannot draw any further conclusion
277 from this comparison: as widely used as it is, the Turc-Mezentsev relationship
278 remains a theoretical model and cannot be considered superior to the data-based
279 elasticity assessment.

280

281 **5. Results: Regional elasticity analysis over France**

282 Henceforth, we only consider the empirical elasticity estimates given by the GLS2
283 method. Figure 9 illustrates the results: each of the 519 gaging stations of the data
284 set are shown, but the points for which the elasticity coefficient is not significantly
285 different from zero are indicated with a cross only. For the other points, the color
286 code gives the elasticity value.

287 From the maps, it is difficult to identify physical reasons for the spatial variations in
288 elasticity values. The Massif central highlands seem to show a slightly higher
289 occurrence of high-intensity elasticities, both to P and E_P , and the Paris Basin
290 lowlands a slightly lower occurrence. This tendency could perhaps be related to the
291 absence/presence of large groundwater aquifers, but more detailed comparative
292 studies are needed to draw a firm conclusion.

293 A few outliers appear, which is common when using a large data set: one catchment
294 shows a negative elasticity to precipitation and five catchments show a positive
295 elasticity to potential evaporation. We checked each of the plots individually and
296 verified that this was in fact due to a very limited span of streamflow anomaly ΔQ ,
297 which made the regression rather meaningless.

298 To conclude this countrywide analysis of elasticity, we tested a possible relation
299 between catchment size and elasticity values. Figure 10 speaks for itself: over the

300 range of catchment areas covered by this study, no trend could be identified with
301 catchment area.

302

303 **6. Conclusion**

304 **6.1 Synthesis**

305 In this paper, we identified an improved method to assess the empirical elasticity of
306 streamflow to precipitation and potential evaporation. This method (GLS2), which
307 uses long-term hydrometeorological records, was tested on a set of 519 French
308 catchments.

309 We started with a synthetic data set and compared this improved method with the
310 reference nonparametric method and with several univariate and bivariate
311 alternatives: we obtained results with a much lower bias and RMSE, this difference
312 being clearly due to the fact that the improved method was able to account for the
313 covariation of precipitation and potential evaporation anomalies.

314 We then compared the improved empirical elasticity estimate with the theoretical
315 estimates derived analytically from the Turc-Mezentsev formula. Empirical and
316 theoretical estimates weakly correlated: the link between the two measurements on a
317 catchment-by-catchment basis is weak for precipitation, and very weak for potential
318 evaporation.

319

320 **6.2 Limits and perspectives**

321 As a simple method characterizing the sensitivity of streamflow to climatic changes,
322 the identification of empirical elasticity seems promising. Indeed, the empirical
323 elasticity assessment advocated in this paper can provide an estimate of the impact
324 of climate change on hydrology that is *almost* model-free (except for the assumption
325 of linearity, of course) and allows digging into *past* observations to predict the impact
326 of *future* changes. Another perspective can also be seen for studies involving
327 hydrological models for climate change assessment: empirical elasticity could
328 provide a very useful benchmark against which to test the predictions of complex
329 hydrological models (see e.g. how the extrapolation capacity of several hydrological
330 models was assessed in Coron et al. (2014)).

331 Naturally, the elasticity assessment has its limits: there is no guarantee for its ability
332 to extrapolate to the most extreme climatic changes (i.e., to changes that are far from
333 those observed over historical records). The formula chosen to compute potential
334 evaporation is also a concern. In this paper, we used the Penman-Shuttleworth
335 equation (Shuttleworth, 1993). We also repeated this study with the Oudin et al.
336 (2005) formula (a formula widely used in France), and the Penman-Monteith equation
337 (Allen et al., 1998), which did not yield significant differences. This result was
338 expected because the catchments considered here are energy-limited with few cases
339 where actual evaporation reaches its potential value. However, for other climates
340 (i.e., drier environments), additional work would be required to further test the
341 sensitivity of streamflow elasticity to the potential evaporation formula.

342

343 **7. Acknowledgements**

344 The authors would like to acknowledge Météo-France for making the SAFRAN
345 meteorological archive available for this study, and SCHAPI-Banque Hydro for the
346 hydrometrical series. They would also like to acknowledge the reviews of Alberto
347 Viglione, Francis Chiew, Tim McVicar and an anonymous reviewer, which contributed
348 to improve this paper.

349

350 **8. References**

- 351 Allen, R., Pereira, L., Raes, D., Smith, M., 1998. Crop evapotranspiration -
352 Guidelines for computing crop water requirements. FAO Irrigation and
353 Drainage paper 56. FAO, Rome, 100 pp.
354 Arora, V.K., 2002. The use of the aridity index to assess climate change effect on
355 annual runoff. J. Hydrol., 265: 164-177.
356 Chiew, F., 2006. Estimation of rainfall elasticity of streamflow in Australia.
357 Hydrological Sciences Journal-Journal Des Sciences Hydrologiques, 51(4):
358 613-625.
359 Chiew, F. et al., 2013. Observed hydrologic non-stationarity in far south-eastern
360 Australia: implications for modelling and prediction. Stochastic Environmental
361 Research and Risk Assessment
362 DOI 10.1007/s00477-013-0755-5.
363 Coron, L., Andréassian, V., Perrin, C., Bourqui, M., Hendrickx, F., 2014. On the lack
364 of robustness of hydrologic models regarding water balance simulation – a
365 diagnostic approach on 20 mountainous catchments using three models of
366 increasing complexity. Hydrology and Earth System Sciences, 18: 727-746.

- 367 Donohue, R., Roderick, M., McVicar, T., 2011. Assessing the differences in
368 sensitivities of runoff to changes in climatic conditions across a large basin. *J.
369 Hydrol.*, 406(3-4): 234-244.
- 370 Donohue, R.J., McVicar, T.R., Roderick, M.L., 2010. Assessing the ability of potential
371 evaporation formulations to capture the dynamics in evaporative demand
372 within a changing climate. *J. Hydrol.*, 386(1-4): 186-197.
- 373 Dooge, J., 1992. Sensitivity of runoff to climate change: a Hortonian approach. *Bull.
374 Amer. Meteol. Soc.*, 73(12): 2013-2024.
- 375 Efron, B., Tibshirani, R., 1994. An introduction to the bootstrap. CRC press, Boca
376 Raton.
- 377 Fu, G., Charles, S.P., Chiew, F., 2007a. A two-parameter climate elasticity of
378 streamflow index to assess climate change effects on annual streamflow.
379 *Water Resour. Res.*, 43, W11419: 1-12.
- 380 Fu, G., Charles, S.P., Viney, N.R., Chen, S., Wu, J.Q., 2007b. Impacts of climate
381 variability on stream-flow in the Yellow River. *Hydrological Processes*, 21(25):
382 3431-3439.
- 383 Johnston, J., 1972. Econometric methods. McGraw-Hill, New York, 437 pp.
- 384 Le Moine, N., Andréassian, V., Perrin, C., Michel, C., 2007. How can rainfall-runoff
385 models handle intercatchment groundwater flows? Theoretical study over
386 1040 French catchments. *Water Resour. Res.*, 43: W06428,
387 doi:10.1029/2006WR005608.
- 388 Lebecherel, L., Andréassian, V., Perrin, C., 2013. On regionalizing the Turc-
389 Mezentsev water balance formula. *Water Resour. Res.*, 49.
- 390 Mezentsev, V., 1955. Back to the computation of total evaporation (Ещё раз о
391 расчете среднего суммарного испарения). *Meteorologiya i Gidrologiya -
392 Meteorology and Hydrology*, 5: 24-26.
- 393 Nelder, J., Mead, R., 1965. A simplex method for function minimization. *Computer
394 Journal*, 7(4): 308-313.
- 395 Nemec, J., Schaake, J., 1982. Sensitivity of water resources systems to climate
396 variation. *Hydrological Sciences Journal-Journal Des Sciences Hydrologiques*,
397 27(3): 327-343.
- 398 Niemann, J.D., Eltahir, A.B., 2005. Sensitivity of regional hydrology to climate
399 changes, with application to the Illinois River basin. *Water Resour. Res.*, 41:
400 W07014, doi:10.1029/2004WR003893.
- 401 Oudin, L. et al., 2005. Which potential evapotranspiration input for a lumped rainfall-
402 runoff model? Part 2 - Towards a simple and efficient potential
403 evapotranspiration model for rainfall-runoff modelling. *J. Hydrol.*, 303(1-4):
404 290-306.
- 405 Potter, N.J., Chiew, F.H.S., Frost, A.J., 2010. An assessment of the severity of recent
406 reductions in rainfall and runoff in the Murray-Darling Basin. *J. Hydrol.*, 381(1-
407 2): 52-64.
- 408 Potter, N.J., Petheram, C., Zhang, L., 2011. Sensitivity of streamflow to rainfall and
409 temperature in south-east Australia during the Millennium drought, 19th
410 International Congress on Modelling and Simulation. MSSANZ, Perth,
411 Australia.
- 412 Potter, N.J., Zhang, L., 2009. Interannual variability of catchment water balance in
413 Australia. *J. Hydrol.*, 369: 120-129.
- 414 Sankarasubramanian, A., Vogel, R.M., Limbrunner, J.F., 2001. Climate elasticity of
415 streamflow in the United States. *Water Resour. Res.*, 37(6): 1771-1781.

- 416 Schaake, J., Liu, C., 1989. Development and application of simple water balance
417 models to understand the relationship between climate and water resources,
418 New Directions for Surface Water Modeling. IAHS, Wallingford, pp. 343-352.
419 Shuttleworth, W.J., 1993. Evaporation. In: Maidment, D.R. (Ed.), Handbook of
420 hydrology. McGraw-Hill, New-York.
421 Turc, L., 1954. The water balance of soils: relationship between precipitations,
422 evaporation and flow (Le bilan d'eau des sols: relation entre les précipitations,
423 l'évaporation et l'écoulement). Annales Agronomiques, Série A(5): 491-595.
424 Vogel, R.M., Wilson, I., Daly, C., 1999. Regional regression models of annual
425 streamflow for the United States. Journal of Irrigation and Drainage
426 Engineering, 125(3): 148-157.
427 Wolock, D.M., McCabe, G.J., 1999. Estimates of runoff using water-balance and
428 atmospheric general circulation models. Journal of the American Water
429 Resources Association, 35(6): 1341-1350.
430 Yang, H., Yang, D., 2011. Derivation of climate elasticity of runoff to assess the
431 effects of climate change on annual runoff. Water Resour. Res., 47.
432 Yang, H., Yang, D., Hu, Q., 2014. An error analysis of the Budyko hypothesis for
433 assessing the contribution of climate change to runoff. Water Resour. Res.,
434 50: 9620-9629.
435 Yang, H., Yang, D., Lei, Z., Sun, F., 2008. New analytical derivation of the mean
436 annual water-energy balance equation. Water Resour. Res., 44: W03410,
437 doi:10.1029/2007WR006135.
438
439
440

441 Appendix 1 – GLS regression

442 The parameters of the GLS regression were inferred by maximizing the log-likelihood
 443 function associated with this model:

$$L\left(\{\Delta Q_i^{(M)}\}, \{\Delta X_i^{(M)}\} | e_{Q/X}^{(M)}, \sigma, \alpha\right) = -\frac{k}{2} \log(2\pi) - k \log(\sigma) - \frac{1}{2} \log(1-\alpha^2) - \frac{1}{2\sigma^2} \left((1-\alpha^2)\omega_1^2 + \sum_{i=2}^k (\omega_i - \alpha\omega_{i-1})^2 \right) \quad \text{Eq. 9}$$

444 where k is the number of sub-periods. The optimization was performed with the
 445 Nelder-Mead algorithm (Nelder and Mead, 1965) using the ordinary least-square
 446 solution (OLS) as a starting point (i.e., the solution of the same regression model with
 447 $\alpha = 0$). The validity of the model assumptions was checked (see Appendix 2) by
 448 computing the Shapiro-Wilks test (with an expected p -value greater than 0.05) and
 449 Durbin-Watson statistic (with an expected value greater than 1) from the series of
 450 innovations $\hat{\delta}_i$:

$$\hat{\delta}_i = \hat{\omega}_i - \alpha\hat{\omega}_{i-1} \text{ if } i > 1 \text{ and } \hat{\delta}_1 = \hat{\omega}_1 \quad \text{Eq. 10}$$

$$\hat{\omega}_i = \Delta Q_i^{(M)} - e_{Q/X}^{(M)} \Delta X_i^{(M)} \quad \text{Eq. 11}$$

451 Unlike the OLS solution, the distribution of the elasticity values obtained with this
 452 approach does not have a closed form. As a result, the significance of the
 453 regression's coefficients was assessed with a bootstrap approach as follows:

454 a. The GLS model was fit with the maximum likelihood approach first. This
 455 allowed computing the series of innovations δ_i .

456 b. The innovations $\{\delta_i\}_{i=2,\dots,n}$ were resampled with replacement to form a new
 457 series of bootstrapped innovations $\{\delta_i^*\}_{i=2,\dots,n}$. The first innovation δ_1^* of this
 458 series was set to ω_1 .

459 c. The bootstrapped innovations were used to generate a new series of
 460 bootstrapped observations $\Delta Q_i^{(M)*} = e_{Q/X}^{(M)} \Delta X_i + \sum_{i=1}^n \delta_i^* \alpha^i$.

461 d. Finally the GLS model was fit with the maximum likelihood approach using the
 462 bootstrapped observations leading to new values of the GLS parameters.
 463 Steps (c) and (d) were repeated 1000 times and the 2.5% and 97.5% percentiles of
 464 the GLS parameters were derived from the empirical distribution formed with the

465 1000 parameter samples. A parameter was considered as significantly different from
466 zero if both the 2.5% and 97.5% percentiles were either strictly positive or negative.

467

468

469 **Appendix 2 - Validity of statistical assumptions underlying the**
470 **regression models**

471 This section reviews the validity of the statistical assumptions underlying the OLS2
472 and GLS2 regression models described in section 3.3.

- 473 • Figure 11.a shows that the GLS2 model has the highest proportion of
474 catchments where the normality assumption cannot be rejected based on the
475 Shapiro-Wilks test. However, the difference with the other models remains
476 limited, with this proportion varying from 50% for OLS2 with 10-year sub-
477 periods to 63% for GLS2 with 20-year sub-periods. Overall, a significant
478 proportion of catchments still fail the test, whatever regression model is
479 considered, which suggests that additional assumptions could be tested for
480 the distribution of the innovations.
- 481 • Figure 11.b reveals that a high level of autocorrelation is present in the
482 innovations of the OLS2 model with only 5% (with 10-year sub-periods) and
483 only 27% (with 20-year sub-periods) of the catchments reaching a satisfactory
484 Durbin-Watson statistic value. This was an expected result. Logically, this
485 proportion is much higher for the GLS2 models, reaching 89% for 10-year sub-
486 periods and 84% for 20-year sub-periods. Here also a small proportion of the
487 catchments fail the test, even with regression models embedding an explicit
488 autocorrelation treatment. This result suggests that the residuals may require
489 higher-order autoregressive models.

490

491 Overall, the results illustrated in Figure 11 indicate that the GLS2 model is the most
492 satisfactory regression model from a statistical point of view. The difference
493 introduced by the length of the averaging period (10 or 20 years) is very limited.

494

495 Appendix 3 – Main characteristics of the catchment dataset

496

Catchment code	e_{Q/E_p}	$e_{Q/P}$	Altitude of the outlet (m a.s.l.)	Area (km ²)	River Name
A1050310	-0.74	0.58	282	238	L' Ill à Altkirch
A1080330	-0.58	0.54	242	668	L' Ill à Didenheim
A1152010	-0.42	0.48	256	288	La Largue à Illfurth
A2023030	-0.58	0.54	432	44	La Petite Fecht à Stosswihr
A2073010	-0.38	0.86	303	31	Le Strengbach à Ribeauvillé
A2122010	0.05	0.68	326	118	La Weiss à Kaysersberg [Fréland-Gare]
A2332110	-0.52	0.69	262	107	La Lièpvrette à Lièpvre
A2512010	-1.25	0.91	221	42	L' Andlau à Andlau
A2612010	-0.60	0.71	161	57	L' Ehn à Niedernai
A2732010	-1.31	1.08	267	224	La Bruche à Russ [Wisches]
A2842010	0.04	1.01	169	167	La Mossig à Soultz-les-Bains
A3151010	-0.22	0.66	146	280	La Moder à Schweighouse-sur-Moder [amont]
A3301010	-0.37	0.52	144	622	La Moder à Schweighouse-sur-Moder [aval]
A3422010	-0.57	0.45	196	184	La Zorn à Saverne [Schinderthal]
A3472010	0.23	0.80	147	684	La Zorn à Waltenheim-sur-Zorn
A3712010	-0.84	0.41	176	192	La Sauer à Goersdorf [Liebfraenthal]
A3832010	-0.59	0.78	124	204	Le Seltzbach à Niederroedern
A3902010	-0.64	0.38	173	275	La Lauter à Wissembourg [Weiler]
A4050620	-0.98	1.73	439	152	La Moselle à Rupt-sur-Moselle
A4142010	-0.58	1.11	407	184	La Moselotte à Vagney [Zainvillers]
A4173010	-0.61	0.98	455	65	La Cleurie à Cleurie
A4200630	-0.71	0.99	372	627	La Moselle à Saint-Nabord [Noirgueux]
A4250640	-0.88	0.90	325	1218	La Moselle à Épinal
A5261010	-0.72	0.74	265	383	Le Madon à Mirecourt
A5431010	-0.31	0.77	225	948	Le Madon à Pulligny
A5730610	-0.38	0.88	200	3346	La Moselle à Toul
A6051020	-0.51	0.59	339	371	La Meurthe à Saint-Dié
A6151030	-0.70	0.51	282	727	La Meurthe à Raon-l'Étape
A6571110	-0.18	0.81	220	560	La Vezouze à Lunéville
A6731220	-0.45	0.75	234	498	La Mortagne à Gerbéviller
A6761010	-0.52	0.96	211	2294	La Meurthe à Damelevières
A6953010	-0.18	1.32	198	85	L' Amézule à Lay-Saint-Christophe
A7010610	-0.54	0.90	184	6835	La Moselle à Custines
A7122010	-0.16	0.73	187	228	L' Esch à Jezainville
A7642010	-0.41	0.41	200	150	La Petite Seille à Château-Salins
A7821010	-0.22	0.71	180	928	La Seille à Nomeny
A7881010	-0.16	0.67	164	1274	La Seille à Metz
A8431010	0.06	1.17	167	1241	L' Orne à Rosselange
A9942010	-0.39	0.72	191	1150	La Nied à Bouzonville
B0220010	-0.18	0.65	300	368	La Meuse à Goncourt
B1092010	-1.02	0.40	291	401	Le Mouzon à Circourt-sur-Mouzon [Villars]

B2220010	-0.46	0.75	216	2543	La Meuse à Saint-Mihiel
B3150020	-0.59	0.84	162	3915	La Meuse à Stenay
B4631010	-0.26	0.74	159	1978	La Chiers à Carignan
B5322010	0.00	0.77	153	125	La Vence à la Francheville
D0206010	0.06	0.79	133	115	La Solre à Ferrière-la-Grande
E1766010	-0.15	0.26	37	88	La Rhonelle à Aulnoy-lez-Valenciennes
E1827020	-0.31	0.99	15	241	L' Hognau à Thivencelle
E3346010	-0.35	0.45	26	132	La Marque à Bouvines
E3511210	-1.45	0.81	83	87	La Lys à Lugy
E4035710	0.12	0.79	19	392	L' Aa à Wizernes
E5300210	-0.90	0.73	26	103	La Liane à Wirwignes
E5400310	-0.08	0.44	6	917	La Canche à Brimeux
E5406510	-0.08	0.55	24	345	La Ternoise à Hesdin
E5505720	0.06	0.36	12	792	L' Authie à Dompierre-sur-Authie
E6470910	0.08	0.34	4	5643	La Somme à Abbeville [Epagne-Epagnette]
G1003010	-0.58	0.69	15	255	L' Yères à Touffreville-sur-Eu
H0100010	-0.57	0.67	249	373	La Seine à Nod-sur-Seine
H0100020	-1.07	0.87	180	686	La Seine à Plaines-Saint-Lange
H0400010	-0.24	0.66	149	2340	La Seine à Bar-sur-Seine
H0400020	-0.13	0.60	139	2392	La Seine à Courtenot
H0503010	-0.09	0.64	109	249	L' Hozain à Buchères [Courgerennes]
H1051020	-0.29	0.66	185	690	L' Aube [partielle] à Longchamp-sur-Aujon [Outre Aube]
H1333010	1.62	1.87	137	22	La Laine à Soulaines-Dhuys
H1513210	-0.38	0.72	86	171	La Barbuise à Pouan-les-Vallées
H1603010	-0.21	0.46	78	366	La Superbe à Saint-Saturnin
H1932020	0.04	0.43	63	281	La Voulzie à Jutigny
H2062010	-0.61	0.29	161	264	Le Beuvron à Ouagne [Champmoreau]
H2073110	-1.00	0.40	170	87	Le Sauzay à Corvol-l'Orgueilleux
H2083110	-0.32	0.52	150	192	La Druyes à Surgy
H2322010	-0.49	0.47	312	267	Le Serein à Bierre-lès-Semur
H2342010	-0.35	0.51	129	1116	Le Serein à Chablis
H2412010	-0.20	0.58	205	478	L' Armançon à Quincy-le-Vicomte
H2513110	-0.43	0.75	88	133	Le Tholon à Champvallon
H3102010	-0.39	0.49	187	152	L' Ouanne à Toucy
H3122010	-0.46	0.46	133	559	L' Ouanne à Charny
H3201010	-0.38	0.64	78	2302	Le Loing à Châlette-sur-Loing
H3613010	-0.14	0.22	86	162	Le Lunain à Paley
H3623010	-0.15	0.23	105	104	L' Orvanne à Blennes
H4022020	-0.20	0.19	56	851	L' Essonne à Guigneville-sur-Essonne [La Mothe]
H4223110	-0.16	0.43	80	152	La Remarde à Saint-Cyr-sous-Dourdan
H4243010	-0.18	0.55	54	231	L' Yvette à Villebon-sur-Yvette
H5062010	-0.14	0.76	206	618	Le Rognon à Doulaincourt-Saucourt
H5142610	-0.39	0.79	170	114	La Chée à Villotte-devant-Louppy [Villote devant Loupy]
H5172010	-0.23	0.78	95	2109	La Saulx à Vitry-en-Perthois
H5732010	-0.06	0.84	62	769	Le Grand Morin à Pommeuse
H6102010	-0.63	0.73	222	283	L' Aire à Beausite [Amblaincourt]
H6122010	-0.56	0.97	154	629	L' Aire à Varennes-en-Argonne

H6162010	-0.40	0.92	117	957	L' Aire à Chevières
H6201010	-0.44	0.78	100	2242	L' Aisne à Mouron
H6221010	-0.48	0.84	77	2888	L' Aisne à Givry
H6313020	-0.19	0.27	59	810	La Suippe à Orainville
H6423010	-0.05	0.58	58	300	L' Ardres à Fismes
H6531011	-0.23	0.57	33	7810	L' Aisne à Trosly-Breuil [Hérant]
H7021010	-0.09	0.59	160	320	L' Oise à Hirson
H7033010	-0.95	0.90	140	256	Le Thon à Origny-en-Thiérache
H7041010	-0.27	0.85	101	860	L' Oise à Monceau-sur-Oise
H7061010	-0.35	0.80	70	1193	L' Oise à Origny-Sainte-Benoite
H7162010	-0.17	0.85	51	1637	La Serre à Pont à Bucy
H7401010	-0.21	0.57	35	4320	L' Oise à Sempigny
H7423710	-0.24	0.36	33	280	L' Aronde à Clairoix
H7611012	-0.14	0.60	26	13484	L' Oise à Pont-Sainte-Maxence [Sarron]
H7713010	-0.52	0.31	89	214	Le Petit Thérain à Saint-Omer-en-Chaussée
H7742010	-0.82	0.68	61	755	Le Thérain à Beauvais
H7742020	-0.25	0.42	33	1210	Le Thérain à Maysel
H7833520	0.05	0.09	32	58	L' Ysieux à Viarmes [Giez]
H7853010	-0.23	0.22	37	102	Le Sausseron à Nesles-la-Vallée
H8012010	-0.66	0.63	87	247	L' Epte à Gournay-en-Bray
H8043310	0.02	-0.01	40	99	L' Aubette de Magny à Ambleville
H8212010	-0.45	0.53	53	377	L' Andelle à Vascoeuil
H9202010	0.15	0.44	119	477	L' Avre à Acon
H9222010	0.12	0.35	78	872	L' Avre à Muzy
H9331010	0.08	0.28	24	4561	L' Eure à Cailly-sur-Eure
H9402030	-0.15	0.26	47	1029	L' Iton à Normanville
H9501010	-0.13	0.11	13	5891	L' Eure à Louviers
I0113010	-0.17	0.51	166	82	Le Guiel à Montreuil-l'Argillé
I0122010	-0.20	0.47	127	251	La Charentonne à Ferrières-Saint-Hilaire
I1203010	-0.38	0.46	32	173	La Calonne aux Authieux-sur-Calonne
I2001010	-0.41	0.57	90	88	La Dives à Saint-Lambert-sur-Dive
I2021010	-0.37	0.37	53	283	La Dives à Beaumais
I2213610	-0.07	0.52	6	57	L' Ancre à Cricqueville-en-Auge
I3131010	-0.23	0.64	106	1019	L' Orne à Rabodanges
I4032010	-0.76	0.63	8	256	La Seulles à Tierceville
I5053010	1.15	0.24	76	116	La Souleuvre à Carville
I7222020	0.47	1.62	18	141	La Soulles à Saint-Pierre-de-Coutances
I7913610	-0.27	0.70	9	73	Le Thar à Jullouville
J0014010	-1.09	0.44	111	65	Le Nançon à Lécousse [Pont aux Anes]
J0144010	-0.76	0.54	58	82	La Loysance à Saint-Ouen-la-Rouërie
J0323010	-0.42	0.39	19	62	Le Guyoult à Epiniac
J1103010	-0.82	0.61	32	103	L' Arguenon à Jugon-les-Lacs
J1114010	-0.54	0.22	41	113	La Rosette à Mégrit
J1313010	-0.77	0.72	40	244	Le Gouessant à Andel
J1513010	-0.87	0.81	103	135	Le Gouët à Saint-Julien
J1813010	-0.68	0.57	17	342	Le Leff à Quemper-Guézennec
J2233010	-0.74	0.62	94	265	Le Léguer à Belle-Isle-en-Terre

J2603010	-0.48	0.54	26	44	Le Jarlot à Plougonven
J2605410	-0.56	0.51	27	42	Le Tromorgant à Plougonven
J2723010	-0.66	0.74	13	142	La Penze à Taulé [Penhoat]
J3024010	-0.12	0.76	33	45	Le Guillec à Trézilidé
J3205710	-0.13	0.91	39	24	L' Aber Wrac'h au Drennec
J3213020	-0.56	0.81	47	27	L' Aber-Benoit à Plabennec [Loc Maria]
J3323020	-0.36	0.66	20	95	L' Aber Ildut à Brélès [Keringar]
J3601810	-2.25	1.21	97	117	L' Aulne à Scrignac [Le Goask]
J3713010	-0.82	0.65	91	258	L' Hyères à Trébrivan [Pont Neuf]
J3834010	-0.11	0.77	26	140	La Douffine à Saint-Ségal [Kerbriant]
J4214510	-0.88	0.62	128	7	Le Langelin à Briec [Pont D 72]
J4224010	-0.52	0.64	22	108	Le Jet à Ergué-Gabéric
J4313010	-0.25	0.95	20	181	Le Steir à Guengat [Ty Planche]
J4514010	-0.39	0.66	20	21	Le Moros à Concarneau [Pont D 22]
J4614010	-0.72	0.65	36	72	Le Ster Goz à Bannalec [Pont Meya]
J4742010	-0.33	0.74	23	576	L' Éillé à Arzano [Pont Ty Nadan]
J4803010	-1.29	1.14	100	102	L' Isole à Scaër [Stang Boudilin]
J4902010	-0.06	0.90	7	832	La Laïta à Quimperlé [ancienne]
J5102210	-0.54	0.54	24	299	Le Scorff à Plouay [Pont Kerlo]
J5613010	-0.53	0.52	44	316	L' Evel à Guénin
J5704810	-0.73	0.50	46	46	Le Coët-Organ à Quistinic [Kerdec]
J6213010	-0.51	1.05	25	182	Le Loch à Brech
J7083110	-0.40	0.62	44	152	Le Chevré à la Bouëxière [Le Drugeon]
J7483010	-0.32	0.75	17	809	La Seiche à Bruz [Carcé]
J7633010	-0.24	0.89	24	406	Le Semnon à Bain-de-Bretagne [Rochereuil]
J7824010	-0.26	0.76	15	112	L' Aron à Grand-Fougeray [La Bernardais]
J7973010	-0.20	0.90	27	40	Le Canut Sud à Saint-Just [La rivière Colombel]
J8002310	-1.58	1.12	178	29	L' Oust à Saint-Martin-des-Prés [La Ville Rouault]
J8363110	-0.44	0.79	35	301	L' Yvel à Loyat [Pont D 129]
J8433010	-0.49	0.72	49	135	La Cliae à Saint-Jean-Brévelay
J8602410	-0.38	0.57	69	28	L' Aff à Paimpont [Pont du Secret]
J8632410	-0.37	0.68	14	343	L' Aff à Quelneuc [La rivière]
J8813010	-0.42	0.90	26	161	L' Arz à Molac [Le Qinquizio]
J9300610	-0.10	0.54	1	10148	La Vilaine à Rieux
K0010010	0.42	1.48	1116	60	La Loire à Usclades-et-Rieutord [Rieutord]
K0403010	-0.07	1.02	936	138	Le Lignon du Velay au Chambon-sur-Lignon
K0454010	-0.19	0.79	596	217	La Dunières à Sainte-Sigolène [Vaubarlet]
K0523010	-1.02	0.38	706	347	L' Ance du Nord à Saint-Julien-d'Ance [Laprat]
K0567520	-0.48	0.86	653	129	La Semène à Saint-Didier-en-Velay [Le Crouzet]
K0567530	-0.07	0.36	811	58	La Semène à Jonzieux
K0624510	-0.28	0.56	432	105	Le Bonson à Saint-Marcellin-en-Forez [Le Bled]
K0663310	-0.84	1.07	583	61	La Coise à Larajasse [Le Nézel]
K0673310	-0.15	1.05	436	181	La Coise à Saint-Médard-en-Forez [Moulin Brûlé]
K0724510	-0.53	0.65	342	13	Le Chanasson à Civens [La rivière]
K0733220	-1.58	0.63	817	60	Le Lignon de Chalmazel à Chalmazel [Chevelières]
K0773220	-1.15	0.74	333	662	Le Lignon de Chalmazel à Poncins [2]
K0813020	-1.84	1.58	378	197	L' Aix à Saint-Germain-Laval

K0974010	-0.38	0.84	364	86	Le Gand à Neaux
K0983010	-0.47	0.84	293	435	Le Rhins à Saint-Cyr-de-Favières [Pont Mordon]
K1084010	-1.58	0.71	357	23	La Teysonne à Changy [La Noaillerie]
K1173210	5.89	2.39	241	593	L' Arconce à Montceaux-l'Étoile
K1284810	-0.63	0.78	318	135	La Selle à la Celle-en-Morvan [Polroy]
K1321810	-1.25	0.49	268	1792	L' Arroux à Étang-sur-Arroux [Pont du Tacot]
K1503010	-1.69	0.47	361	157	La Besbre à Châtel-Montagne
K1524010	-0.99	0.69	314	121	Le Barbenan au Breuil
K1724210	-1.05	0.80	212	114	La Dragne à Vandenesse
K1753110	-0.91	0.25	200	333	L' Alène à Cercy-la-Tour [Coueron]
K1914510	-0.62	0.63	196	115	L' Ixeure à la Fermeté
K1954010	-0.68	0.64	207	226	La Nièvre d'Arzembouy à Poiseux [Poisson]
K2064010	-0.86	1.28	910	66	Le Langouyrou à Langogne
K2123010	-0.66	0.89	1124	125	Le Chapeauroux à Châteauneuf-de-Randon [Hermet]
K2233020	-0.35	1.37	634	231	L' Ance du Sud à Monistrol-d'Allier [Pouzas]
K2514010	-0.08	1.13	768	156	L' Allanche à Joursac [Pont du Vernet]
K2523010	-0.06	0.93	710	322	L' Alagnon à Joursac [Le Vialard]
K2834010	-0.38	0.83	836	71	La Dolore à Saint-Bonnet-le-Chastel [Moulin Neuf]
K2871910	-1.12	0.56	412	795	La Dore à Saint-Gervais-sous-Meymont [Maison du Parc / Giroux-Dore]
K2884010	-2.87	0.74	403	73	La Faye à Olliergues [Giroux-Faye]
K2944010	-1.66	0.65	335	72	Le Couzon à Courpière [Le Salet]
K3206010	-3.04	-0.31	784	8	La source-de-chez-Pierre à Ceyssat
K3222010	-0.70	0.68	666	360	La Sioule à Pontgibaud
K3264010	-0.57	0.70	538	111	La Saunade à Pontaumur
K3292020	-0.74	0.65	502	1300	La Sioule à Saint-Priest-des-Champs [Fades-Besserve]
K4094010	-0.50	0.41	153	478	Le Nohain à Saint-Martin-sur-Nohain [Villiers]
K4443010	-0.30	0.59	79	165	L' Ardoux à Lailly-en-Val
K4873110	-0.01	0.56	82	263	La Brenne à Villedômer [Bas-Villaumay]
K5090910	-0.21	0.69	321	526	Le Cher à Chambonchard
K5183010	-0.41	0.54	329	861	La Tardes à Évaux-les-Bains
K6334010	-0.54	0.01	180	79	La Nère à Aubigny-sur-Nère
K6402510	-0.80	0.06	102	1240	La Sauldre à Salbris
K6492510	-0.85	0.30	73	2297	La Sauldre à Selles-sur-Cher
K7312610	-0.90	0.65	82	1707	L' Indre à Saint-Cyran-du-Jambot
K7414010	-0.47	0.60	99	109	La Tourmente à Villeloin-Coulangé [Coulangé]
K7424010	-0.30	0.51	97	78	L' Olivet à Beaumont-Village [1]
K7514010	-0.20	0.69	66	128	L' Échandon à Saint-Branchs
L0010610	-1.15	0.68	749	64	La Vienne à Peyrelevade [Servières]
L0010620	-1.43	0.68	740	77	La Vienne à Peyrelevade [La Rigole du Diable]
L0093010	-0.27	0.96	301	188	La Combade à Masléon
L0314010	-0.95	0.71	313	131	La Vige à Saint-Martin-Sainte-Catherine
L0563010	-0.77	0.72	218	605	La Briance à Condat-sur-Vienne [Chambon Veyrinas]
L0624010	-0.45	0.76	230	153	L' Aixette à Aixe-sur-Vienne
L0813010	-0.59	0.76	214	298	La Glane à Saint-Junien [Le Dérot]
L4033010	-0.53	0.84	448	190	La Rozeille à Moutier-Rozeille [Aubusson]
L4220710	-0.67	0.60	215	1235	La Creuse à Fresselines
L4321710	-0.62	0.49	272	561	La Petite Creuse à Genouillac

L4411710	-0.59	0.57	218	853	La Petite Creuse à Fresselines [Puy Rageaud]
L4530710	-0.73	0.54	187	2427	La Creuse à Éguzon-Chantôme
L4653010	-0.63	0.60	124	438	La Bouzanne à Velles [Forges]
L5034010	-1.37	0.52	324	129	L' Ardour à Folles [Forgefer]
L5101810	-0.64	0.59	297	568	La Gartempe à Folles [Bessines]
L5134010	-0.57	1.00	200	175	La Semme à Droux
L5223020	-0.44	0.75	178	286	Le Vincou à Bellac [2]
L5323010	-0.39	0.65	171	232	La Brame à Oradour-Saint-Genest
L5623010	-0.72	1.01	183	188	La Benaize à Jouac
L6202030	-0.56	0.48	58	886	La Claise au Grand-Pressigny [Étableau 2]
M0050620	-0.08	0.71	124	909	La Sarthe à Saint-Céneri-le-Gérei [Moulin du Désert]
M0250610	-0.13	0.73	48	2713	La Sarthe à Neuville-sur-Sarthe [Montreuil]
M0361510	-0.15	0.43	102	833	L' Huisne à Nogent-le-Rotrou [Pont de bois]
M0500610	0.03	0.55	38	5452	La Sarthe à Spay [amont]
M0680610	-0.16	0.64	21	7523	La Sarthe à Saint-Denis-d'Anjou [Beffes]
M1034020	0.05	0.71	126	267	L' Ozanne à Trizay-lès-Bonneval [Prémoteux]
M1041610	-0.11	0.89	118	1080	Le Loir à Saint-Maur-sur-le-Loir
M1214010	-0.13	0.33	121	87	Le Couëtron à Souday [Glatigny]
M3253110	-0.79	0.97	94	185	L' Aron à Moulay
M3313010	-1.12	0.69	115	121	L' Ernée à Ernée
M3323010	-0.66	0.76	67	376	L' Ernée à Andouillé [Les Vaugeois]
M3340910	-0.25	0.88	45	2908	La Mayenne à l' Huisserie [Bonne]
M3423010	-0.24	0.78	50	404	La Jouanne à Forcé
M3504010	-0.55	0.83	51	234	Le Vicoin à Nuillé-sur-Vicoin
M3600910	-0.26	0.96	27	3935	La Mayenne à Château-Gontier
M3630910	-0.08	0.87	20	4166	La Mayenne à Chambellay
M3774010	-0.60	0.76	43	77	Le Chéran à la Boissière
M5102010	-0.23	0.87	46	259	Le Layon à Saint-Georges-sur-Layon
M5222010	-0.26	0.79	20	927	Le Layon à Saint-Lambert-du-Lattay [Pont de Bézigon]
M6014010	-0.14	0.78	70	38	Le Beuvron à Andrezé [Tuvache]
M6333020	-0.32	0.67	6	463	L' Erdre à Nort-sur-Erdre [Moulin de Vault]
M7112410	-0.54	0.63	50	872	La Sèvre Nantaise à Tiffauges [La Moulinette]
M7453010	-0.67	0.60	19	595	La Maine à Remouillé
M8205020	-0.02	1.11	6	139	L' Ognon aux Sorinières [Villeneuve]
N0113010	0.29	0.89	28	33	Le Falleron à Falleron
N3001610	-0.30	0.69	65	131	Le Grand Lay à Saint-Prouant [Monsireigne]
N3024010	-0.52	0.52	42	121	Le Louing à Chantonnay [St-Philbert du Pont Charrault]
O0015310	1.36	1.32	558	36	Le Maudan à Fos
O0105110	-2.23	-0.18	2154	5	La Neste de Cap de Long à Aragnouet [Les Edelweiss]
O0126210	-1.31	0.90	1070	67	La Neste de Rioumajou à Tramezaïgues [Maison Blanche]
O0362510	-0.82	0.62	472	385	Le Salat à Soueix-Rogalle [Kercabanac]
O0384010	-1.10	0.52	501	170	L' Arac à Soulac [Freychet]
O0502520	-1.18	0.61	386	1159	Le Salat à Saint-Lizier [Saint Girons]
O0525010	0.02	1.16	441	14	La Gouarège à Cazavet [Aliou]
O0592510	-0.45	0.72	270	1579	Le Salat à Roquefort-sur-Garonne
O0744030	-0.84	0.86	290	220	L' Arize au Mas-d'Azil
O1115010	-0.79	0.93	1239	24	L' Artigue à Auzat [Cibelle]

O1432930	-0.71	0.39	521	134	L' Hers à Bélestà [source de Fontestorbes]
O1442910	-0.81	0.73	417	191	L' Hers Vif au Peyrat
O1484310	-1.10	1.01	507	68	La Touyre à Lavelanet [2]
O1494330	-1.03	0.96	387	95	La Touyre à Léran
O1584610	-0.44	0.69	306	136	Le Douctouyre à Vira [Engraviès]
O1634010	-0.35	0.65	239	197	La Vixière à Belpech
O2344010	-0.50	0.71	122	524	Le Girou à Cépet
O2725010	-0.17	0.61	191	36	La Lauze à Sémezies-Cachan [Faget-Abbatial]
O3006710	-0.59	0.83	1026	10	La Goudech à Saint-Maurice-de-Ventalon [La Cépède]
O3011010	-0.43	0.73	927	65	Le Tarn au Pont-de-Montvert [Fontchalettes]
O3035210	1.48	0.88	611	26	Le Briançon aux Bondons [Cocures]
O3064010	-0.51	1.68	554	132	Le Tarnon à Florac
O3084320	1.00	1.13	556	126	La Mimente à Florac
O3165010	-0.59	1.64	708	34	La Brèze à Meyrueis
O3194010	0.34	1.45	704	98	La Jonte à Meyrueis [aval]
O3364010	-0.74	0.77	446	428	La Dourbie à Nant [Pont de Gardies]
O3401010	-0.27	0.98	355	2143	Le Tarn à Millau [2]
O3424010	-1.23	0.49	343	169	Le Cernon à Saint-Georges-de-Luzençon [aval]
O3454310	0.02	0.45	340	112	La Muze à Montjaux [Saint-Hippolyte]
O4194310	-0.23	0.40	357	207	Le Gijou à Vabre [Rocalé]
O4704030	-0.61	0.63	427	71	Le Dadou à Paulinet [Saint-Jean-de-Jeanne]
O5042510	-0.95	0.34	578	300	L' Aveyron à Palmas [Pont de Manson]
O5055010	-0.56	0.47	584	108	Le Serre à Coussergues [Resuenhe]
O5092520	-1.22	0.46	533	584	L' Aveyron à Onet-le-Château [Rodez]
O5192520	-0.80	0.51	276	1060	L' Aveyron à Villefranche-de-Rouergue [Recoules]
O5224010	-0.29	0.74	276	208	L' Alzou à Villefranche-de-Rouergue [barrage Cabal]
O5284310	-0.94	0.59	317	104	La Serène à Saint-André-de-Najac [Canabral]
O5292510	-0.75	0.56	163	1604	L' Aveyron à Laguépie [1]
O5312910	-0.24	0.94	730	139	Le Viaur à Arques
O5344010	-0.11	0.84	814	57	Le Vioulou à Salles-Curan [Trébons-Bas]
O5424010	-1.13	0.42	352	161	Le Céor à Centrès [Estrebaldie]
O5464310	-1.23	0.43	363	176	Le Giffou à Saint-Just-sur-Viaur [La Fabrèguerie]
O5534010	-0.80	0.95	245	223	Le Lézert à Saint-Julien-du-Puy [Port de la Besse]
O5685010	-0.43	0.35	139	181	La Bonnette à Saint-Antonin-Noble-Val
O5754020	-0.53	0.60	125	310	La Vère à Bruniquel [La Gauterie]
O6125010	-0.08	0.90	143	62	La Petite Barguelonne à Montcuq
O6134010	-0.30	0.75	74	453	La Barguelonne à Valence [Fourquet]
O6793310	-0.16	0.58	58	834	La Gélise à Mézin [Courbian]
O6804630	-0.43	0.87	245	9	L' Osse à Castex [Mielan]
O7011510	-0.85	0.90	813	187	Le Lot à Sainte-Hélène
O7015810	-0.57	-0.64	981	33	L' Esclancide à Pelouse [Les Salces]
O7041510	-1.22	0.71	667	468	Le Lot à Balsièges [Bramonas]
O7085010	-0.56	-0.52	663	83	Le Coulagnet à Marvejols
O7101510	-0.94	0.64	525	1158	Le Lot à Banassac [La Mothe]
O7131510	-0.70	0.54	388	1633	Le Lot à Lassouts [Castelnau]
O7145220	0.62	0.91	439	53	La Boralde de Saint-Chély à Castelnau-de-Mandailles
O7234010	-0.46	0.81	948	117	La Rimeize à Rimeize

07245010	-0.08	0.83	947	65	Le Chapouillet à Rimeize [Chassignoles]
07265010	-0.60	0.67	921	78	La Limagnole à Fontans [Saint-Alban]
07444010	-0.78	1.13	924	286	Le Bès à Saint-Juéry
07502510	-0.43	0.70	704	1795	La Truyère à Neuvéglise [Grandval]
07635010	-1.08	0.87	645	109	La Bromme à Brommat
07874010	-1.22	0.33	236	545	Le Dourdou à Conques
08113510	-0.11	0.59	183	681	Le Célé à Figeac [Merlançon]
08133520	-0.62	1.20	142	1246	Le Célé à Orniac [Les Amis du Célé]
08255010	-0.92	0.80	103	119	Le Vert à Labastide-du-Vert [Les Campagnes]
08394310	-0.64	0.45	87	220	La Lémance à Cuzorn
09196210	-0.07	0.42	53	10	La Cadanne à Pondaurat
P0010010	-2.40	0.65	786	89	La Dordogne à Saint-Sauves-d'Auvergne
P0115010	-0.30	0.89	905	21	La Burande à la Tour-d'Auvergne
P0115020	-0.50	0.94	569	85	La Burande [ou ru de Burons] à Singles
P0212510	-0.84	0.68	954	40	La Rhue à Égliseneuve-d'Entraigues
P0364010	-0.63	0.95	709	169	La Santoire à Condat [Roche-Pointue]
P0885010	-1.74	0.61	377	117	Le Mars à Bassignac [Vendes]
P0924010	-0.96	0.64	631	79	La Triouzoune à Saint-Angel
P1114010	-0.48	0.61	566	81	La Luzège à Maussac [Pont de Maussac]
P1154010	-1.11	0.83	452	250	La Luzège à Lamazière-Basse [Pont de Bouyges]
P1502510	-0.52	1.02	419	455	La Maronne à Pleaux [Enchanet]
P1772910	-1.07	0.72	559	349	La Cère à Sansac-de-Marmiesse
P2114010	-2.05	0.67	131	63	La Sourdoire à la Chapelle-aux-Saints
P2184310	-0.68	0.67	114	191	La Tourmente à Saint-Denis-lès-Martel
P2484010	-0.48	0.41	77	573	Le Céou à Saint-Cybranet
P3001010	-1.48	0.74	773	42	La Vézère à Saint-Merd-les-Oussines [Maisonnial]
P3021010	-0.99	0.95	675	138	La Vézère à Bugeat
P3234010	-1.57	0.56	153	104	La Loyre à Voutezac [Pont de l'Aumonerie]
P3245010	-1.03	0.47	123	52	Le Mayne à Saint-Cyr-la-Roche
P3352510	-0.86	0.37	478	164	La Corrèze à Corrèze [Pont de Neupont]
P3502510	-1.06	0.72	224	354	La Corrèze à Tulle [Pont des soldats]
P3614010	-0.47	0.67	546	42	La Montane à Eyrein [Pont du Geai]
P3922510	-0.42	0.81	103	954	La Corrèze à Brive-la-Gaillarde [Le Prieur]
P4015010	-1.38	0.75	133	58	La Couze à Chasteaux [Le Soulier]
P4271010	-0.56	0.66	56	3657	La Vézère à Campagne
P5404010	-0.27	0.65	36	74	L' Eyraud à la Force [Bitarel]
P6081510	-0.85	0.75	137	448	L' Isle à Corgnac-sur-l'Isle
P6134010	-0.54	0.56	154	197	La Loue à Saint-Médard-d'Excideuil
P7001510	-0.80	0.78	91	1859	L' Isle à Bassilac [Charrieras]
P7181510	0.26	0.49	36	3342	L' Isle à Saint-Laurent-des-Hommes [Bénévent]
P7261510	-0.59	0.50	7	3757	L' Isle à Abzac
P8012510	-0.98	1.04	160	140	La Dronne à Saint-Pardoux-la-Rivière [Le Manet]
P8215010	-0.59	0.45	113	40	La Belle à Mareuil
P8312520	-0.66	1.12	37	1912	La Dronne à Bonnes
Q0115710	-1.15	1.52	505	32	L' Oussouet à Trébons
Q0214010	-1.81	0.91	337	78	L' Échez à Louey
Q0280030	-1.75	0.90	167	876	L' Adour à Estirac

Q0664010	-0.28	0.38	141	207	Le Bouès à Juillac
Q1094010	-0.27	1.24	92	426	Le Larcis à Lannux
Q1100010	-0.35	0.91	80	2921	L' Adour à Aire-sur-l'Adour [2]
Q2593310	-0.64	1.07	26	2478	La Midouze à Campagne
Q3120010	-0.33	0.83	6	7707	L' Adour à Saint-Vincent-de-Paul
Q3464010	-0.90	0.96	6	1144	Le Luy à Saint-Pandelon
Q7322510	-3.30	0.85	123	498	Le Saison à Mauléon-Licharre
Q8032510	-0.75	0.77	43	246	La Bidouze à Aïcirits-Camou-Suhast [Saint-Palais]
Q8345910	-0.33	0.75	37	17	Le Mendialçu à Hasparren
Q9164610	-1.89	1.09	149	157	La Nive des Aldudes à Saint-Étienne-de-Baïgorry
R1132510	-1.23	1.34	217	139	La Tardoire à Maisonnais-sur-Tardoire
R1264001	-0.25	0.42	106	293	Le Bandiat à Feuillade
S2224610	-0.42	0.59	41	113	Le Grand Arriou à Moustey [Biganon]
S2235610	-0.29	0.40	35	42	Le Bouron à Belin-Béliet [Moulin du Moine]
S2242510	-0.52	0.70	14	1678	L' Eyre à Salles
S4214010	-1.13	0.34	21	77	Le Magescq à Magescq
S5144010	-1.90	1.37	31	142	La Nivelle à Saint-Pée-sur-Nivelle
U0104010	-0.92	0.86	306	64	Le Coney à Xertigny
U0444310	-0.72	1.41	243	225	La Semouse à Saint-Loup-sur-Semouse
U0474010	-0.57	0.79	209	1028	La Lanterne à Fleurey-lès-Faverney
U0610010	-0.48	0.96	195	3761	La Saône à Ray-sur-Saône
U0635010	-0.18	0.64	200	146	La Gourgeonne à Tincey-et-Pontrebeau
U0724010	-0.92	0.93	200	385	Le Salon à Denèvre
U0924010	-0.48	0.89	232	397	La Vingeanne à Saint-Maurice-sur-Vingeanne
U0924020	-0.55	0.89	198	609	La Vingeanne à Oisilly
U1004010	-1.64	0.42	388	71	L' Ognon à Servance [Fourguenons]
U1025010	-0.89	0.43	445	32	Le Rahin à Plancher-Bas
U1054010	-0.38	0.60	229	1259	L' Ognon à Beaumotte-Aubertans
U1074010	-0.64	0.64	200	1755	L' Ognon à Chevigney-sur-l'Ognon
U1084010	-0.34	0.68	186	2071	L' Ognon à Pesmes
U1109010	-0.52	0.91	291	56	La Venelle à Selongey
U1204010	-0.60	0.87	273	230	La Tille à Crêcey-sur-Tille
U1224010	-0.28	0.66	223	845	La Tille à Arceau [Arcelot]
U1224020	-0.44	0.50	202	882	La Tille à Cessey-sur-Tille
U1235020	-0.66	0.94	194	271	La Norges à Genlis
U1420010	-0.39	0.79	173	11693	La Saône à Pagny-la-Ville [Lechatelet]
U2002010	-0.46	0.70	938	33	Le Doubs à Mouthe
U2012010	-0.24	0.50	855	170	Le Doubs à Labergement-Sainte-Marie
U2022010	-0.27	0.45	824	382	Le Doubs à la Cluse-et-Mijoux [Pontarlier amont]
U2122010	-0.51	0.68	506	1159	Le Doubs à Goumois
U2142010	-0.44	0.67	414	1306	Le Doubs à Glère [Courclavon]
U2215020	-0.62	0.77	394	590	Le Dessoubre à Saint-Hippolyte
U2222010	0.02	0.84	334	2236	Le Doubs à Mathay
U2305210	-1.28	1.10	474	9	Le Saint-Nicolas à Rougemont-le-Château
U2345020	-1.07	0.20	468	30	La Savoureuse à Giromagny
U2345030	-0.87	0.49	358	144	La Savoureuse à Belfort
U2356610	0.00	0.21	323	43	Le Rupt à Dung

U2425260	-0.20	0.16	275	541	Le Cusancin à Baume-les-Dames
U2512010	-0.13	0.87	241	4658	Le Doubs à Besançon
U2542010	-0.49	0.78	201	5169	Le Doubs à Rochefort-sur-Nenon
U2604030	-0.69	1.84	359	291	La Loue à Vuillafans
U2615820	-0.28	0.53	437	210	Le Lison [source] à Nans-sous-Sainte-Anne
U2615830	0.08	0.50	325	284	Le Lison à Myon
U2616410	-0.10	0.42	629	15	Le Verneau à Nans-sous-Sainte-Anne
U2624010	-0.28	1.10	275	1068	La Loue à Chenecey-Buillon
U2634010	-0.28	0.98	236	1264	La Loue à Champagne-sur-Loue
U2722010	-0.32	0.81	180	7346	Le Doubs à Neublans-Abergement
U3205210	-1.26	0.70	368	31	La Grosne à Trades [Les Chambosse]
U3214010	-1.65	0.57	243	334	La Grosne à Jalogny [Cluny]
U3225010	0.87	0.78	214	271	La Guye à Sigy-le-Châtel [Corcelles]
U3424010	-0.26	0.36	176	938	La Seille à Saint-Usuge
U4014010	-0.10	0.49	240	84	La Reyssouze à Montagnat
U4204010	-0.53	0.65	255	41	La Veyle à Lent
U4235010	-0.77	0.71	215	93	Le Renon à Neuville-les-Dames
U4505010	-0.92	0.61	310	55	L' Ardières à Beaujeu
U4624010	-0.77	0.62	211	337	L' Azergues à Châtillon
V0144010	0.03	0.98	606	332	Le Giffre à Taninges [Pressy]
V0205010	-3.49	0.20	458	28	Le Bronze à Bonneville [Thuet]
V0245610	-0.32	0.32	436	47	L' Aire à Saint-Julien-en-Genevois [Thairy]
V0325010	-2.93	0.70	707	171	La Dranse de Morzine à Seytroux [Pont de Couvaloup]
V1015010	-0.88	0.36	851	76	La Valserine à Lélex [Niaizet]
V1015030	-1.63	0.69	579	110	La Valserine à Chézery-Forens [Chézery]
V1015810	-1.32	1.13	401	182	La Semine à Châtillon-en-Michaille [Coz]
V1214010	-7.26	0.89	528	224	Le Fier à Dingy-Saint-Clair
V1235210	-7.92	0.38	469	25	L' Ire à Doussard
V1235610	-3.62	0.24	456	93	L' Eau Morte à Doussard
V1237410	-1.61	0.31	465	30	Le Laudon à Saint-Jorioz
V1264010	-2.70	0.93	316	1286	Le Fier à Vallières
V1414010	-0.26	0.20	382	158	Le Seran à Belmont-Luthézieu [Bavosière]
V1425010	-3.11	2.23	249	41	Le Groin à Artemare [Cerveyrieu]
V1504010	-1.53	0.55	433	94	Le Guiers Mort à Saint-Laurent-du-Pont
V1774010	-0.14	0.68	204	696	La Bourbre à Tignieu-Jameyzieu
V2024010	-1.28	0.60	793	101	La Saine à Foncine-le-Bas
V2035010	-0.33	0.19	819	95	La Lemme à Fort-du-Plasne [Pont-de-Lemme]
V2202010	-0.83	0.82	458	734	L' Ain à Marigny [Chalain]
V2206010	-0.43	0.79	499	51	Le Hérisson à Doucier
V2414010	-2.25	0.83	442	203	La Biènne à Saint-Claude [Chenavier]
V2444020	-0.36	0.94	323	593	La Biènne à Jeurre
V2814020	-0.31	0.37	272	331	Le Suran à Neuville-sur-Ain [La Planche]
V2924010	-0.33	0.64	293	210	L' Albarine à Saint-Rambert-en-Bugey
V2934010	0.01	0.43	242	290	L' Albarine à Saint-Denis-en-Bugey [Pont Saint Denis]
V4144010	-0.20	0.64	309	454	L' Eyrieux à Beauvène [Pont de Chervil]
V4214010	-0.66	0.63	542	189	La Drôme à Luc-en-Diois
V4225010	-1.70	0.76	564	227	Le Bez à Châtillon-en-Diois

V4275010	-0.97	0.56	329	101	La Gervanne à Beaufort-sur-Gervanne
V4414010	-0.43	0.62	276	192	Le Roubion à Soyans
V5045810	-1.20	1.26	638	63	Le Borne à Saint-Laurent-les-Bains [Pont de Nicoulaud]
V6035010	0.42	0.65	338	157	Le Toulourenc à Malaucène [Veaux]
V6052010	-0.94	0.71	194	587	L' Ouvèze à Vaison-la-Romaine
V7124010	0.27	1.28	148	244	Le Gardon de Mialet à Générargues [Roucan]
W0000010	-1.37	0.32	1851	46	L' Isère à Val-d'Isère
W0224010	1.06	1.01	652	333	Le Doron de Bozel à la Perrière [Vignotan]
W2222010	0.50	1.17	750	984	Le Drac à Corps [Le Sautet]
W2335210	-0.23	0.85	948	70	La Roizonne à la Valette [La Rochette]
W2405010	0.54	0.88	885	51	La Jonche à la Mure
W2714010	-0.04	0.66	1088	223	La Romanche à Mizoën [Chambon amont]
W3315010	-0.72	0.23	962	74	Le Meaudret à Méaudre
W3335210	-1.49	0.59	707	37	L' Adouin à Saint-Martin-en-Vercors [Tourtre]
X0010010	0.98	1.44	1363	206	La Durance à Val-des-Prés [Les Alberts]
X0100010	-1.39	0.83	1190	548	La Durance à Briançon [aval]
X0310010	-1.88	0.60	784	2283	La Durance à Embrun [La Clapière]
X0434010	1.46	1.03	1136	542	L' Ubaye à Barcelonnette [Abattoir]
X0454010	1.26	1.27	806	943	L' Ubaye au Lauzet-Ubaye [Roche Rousse]
X0500010	-1.03	0.93	756	3580	La Durance à Espinasses [Serre-Ponçon]
X1034020	-0.14	1.14	674	731	Le Buech à Serres [Les Chambons]
X1225010	-0.01	0.85	829	165	Le Bes à la Javie [Esclangon-Péroure]
X2114010	0.97	0.94	943	138	L' Issole à Saint-André-les-Alpes [Mourefrey]
Y0115410	-1.50	0.96	101	16	La Massane à Argelès-sur-Mer [Mas d'en Tourens]
Y0255020	-0.14	0.65	197	49	L' Ample à Reynès [Le Vila]
Y0325010	0.38	0.78	160	32	La Canterrane à Terrats [Moulin d'en Canterrane]
Y0624020	-0.31	0.02	246	218	L' Agly à Saint-Paul-de-Fenouillet [Clue de la Fou]
Y1225010	0.25	0.07	346	66	Le Lauquet à Greffeil
Y1325010	-0.10	0.46	128	142	Le Treboul à Villepinte
Y1415020	-0.09	0.33	94	242	L' Orbiel à Bouilhonnac [Villedubert]
Y1416210	-0.67	0.84	109	85	La Clamoux à Malves-en-Minervois
Y2015010	0.63	1.21	198	155	L' Arre au Vigan [La Terrisse]
Y2102010	-0.73	0.87	139	916	L' Hérault à Laroque
Y2214010	-0.37	1.06	160	181	La Lergue à Lodève
Y3204010	0.49	1.25	40	116	Le Lez à Montferrier-sur-Lez [Lavalette]
Y4002010	-0.32	0.46	252	50	L' Arc à Pourrières
Y4022010	-0.06	0.56	174	297	L' Arc à Meyreuil [Pont de Bayeux]
Y4214010	-0.46	0.19	96	205	La Touloubre à la Barben [La Savonnière]
Y4604020	0.52	0.55	81	184	Le Gapeau à Solliès-Pont
Y4624010	-0.03	0.83	12	536	Le Gapeau à Hyères [Sainte-Eulalie]
Y5005210	0.47	0.40	254	146	Le Cauron à Bras [Pont de l'Avocade]
Y5032010	-0.74	0.64	183	505	L' Argens à Châteauvert
Y5105010	3.33	1.35	181	203	Le Caramy à Vins-sur-Caramy [Les Marcounious]
Y5106610	1.22	0.86	189	228	L' Issole à Cabasse [Pont des Fées]
Y5202010	-0.73	0.72	42	1651	L' Argens aux Arcs
Y5215020	-0.34	0.92	46	229	L' Aille à Vidauban [Le Baou]
Y5235010	-0.58	0.78	151	194	La Nartuby à Trans-en-Provence

Y5235030	-0.13	0.61	235	149	La Nartuby à Châteaudouble [Rebouillon]
Y5312010	-0.95	0.69	8	2514	L' Argens à Roquebrune-sur-Argens
Y5505410	-3.86	0.72	7	48	Le Grenouiller à Saint-Raphaël [Agay]
Y5615010	-0.11	0.94	133	206	Le Loup à Tourrettes-sur-Loup [Les Vallettes]
Y5615020	-0.06	0.79	192	153	Le Loup à Gourdon [Loup amont]
Y6432010	-0.60	0.96	188	1829	Le Var à Malaussène [La Mescla]
Y6434010	0.19	1.04	140	443	L' Estéron au Broc [La Clave]
Y6624010	-0.16	1.31	280	453	La Roya à Breil-sur-Roya

497

498

499 **Table 1. Summary of the elasticity notations used in this paper (X being precipitation P or**

500 potential evaporation E_P)

Notation	Definition	Formula
$\varepsilon_{Q/X}$	<i>Relative streamflow elasticity – percent change of streamflow Q by percent change of climate variable X</i>	$\frac{\Delta Q}{\bar{Q}} = \varepsilon_{Q/X} \frac{\Delta X}{\bar{X}}$
$e_{Q/X}$	<i>Absolute streamflow elasticity – mm change of streamflow Q by mm change of climate variable X</i>	$\Delta Q = e_{Q/X} \cdot \Delta X$

501

502

503 **Table 2. Comparison of the theoretical and empirical elasticity assessment methods**

	Theoretical (model-based) elasticity assessment	Empirical (data-based) elasticity assessment
Co-variations of different climatic variables	The modeling approach distinguishes between the impact of different climatic variables (by keeping part of the forcing constant while modifying the other part).	Problem: the changes in observed climatic variables can be correlated (e.g., ΔP negatively correlated with ΔT when the driest years are also the warmest), which makes it more difficult to attribute streamflow changes to one or the other variable
Data requirements	No need for long concomitant series of observed streamflow and climatic variables (only what is needed for model calibration)	Long concomitant series of observed streamflow and climatic variables are required
Extrapolation capacity	Extrapolates to extreme climatic changes (i.e., to changes that have not been observed over historical records)	Can only deal with the changes that have been observed in the available historical record.

504

505

506

507 **Table 3. Regression models used to assess empirical elasticity**

Notation	Definition	Inputs	Number of parameters
NP	Nonparametric regression	$\Delta P_i^{(M)}$ or $\Delta E_{P_i}^{(M)}$	0
OLS1	Ordinary least squares using a single climate input	$\Delta P_i^{(M)}$ or $\Delta E_{P_i}^{(M)}$	1
OLS2	Ordinary least squares using two climate inputs	$\Delta P_i^{(M)}$ and $\Delta E_{P_i}^{(M)}$	2
GLS1	Generalized least squares using a single climate input	$\Delta P_i^{(M)}$ or $\Delta E_{P_i}^{(M)}$	3
GLS2	Generalized least squares using two climate inputs	$\Delta P_i^{(M)}$ and $\Delta E_{P_i}^{(M)}$	4

508

509

510 **Table 4. Univariate regression models for empirical elasticity assessment**

$\Delta Q_i^{(M)} = e^{(M)_{Q/X}} \cdot \Delta X_i^{(M)} + \omega_i$		Eq. 12
OLS	$\omega_i \sim N(0, \sigma)$	
GLS	$\begin{cases} \omega_i = \alpha \omega_{i-1} + \delta_i \\ \delta_i \sim N(0, \sigma) \\ \omega_i \sim N(0, \sigma \sqrt{1 - \alpha^2}) \end{cases}$	
$\Delta Q_i^{(M)}$: streamflow anomaly over M years, considered as the explained variable $\Delta X_i^{(M)}$: rainfall or potential evaporation anomaly for the same sub-period, considered as the explanatory variable $e^{(M)_{Q/X}}$: streamflow elasticity (equal to the regression slope) ω_i : regression residual α : parameter of the first-order autoregressive process (AR1) δ_i : innovation of the autoregressive process σ : standard deviation M : number of years over which the long-term streamflow, precipitation and evaporation average is computed		

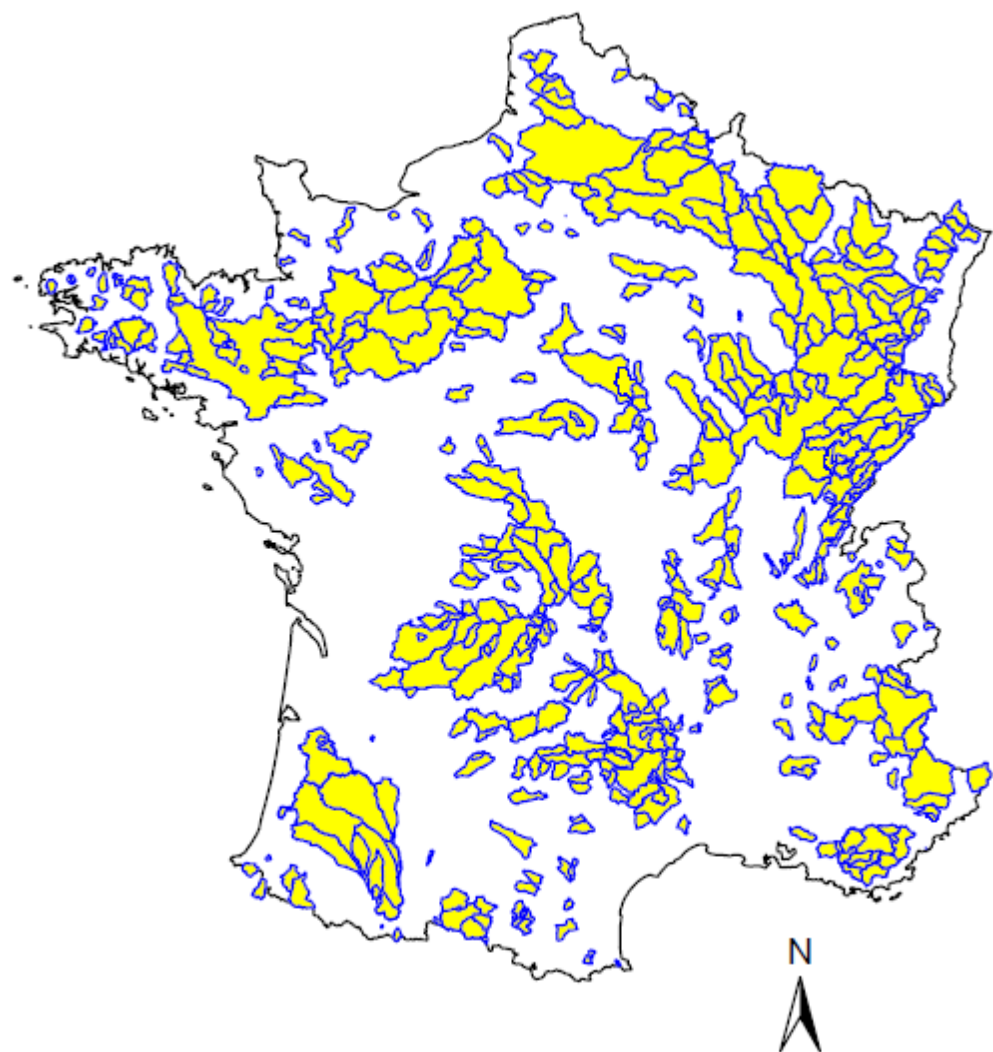
511

512

513 **Table 5. Bivariate regression models for empirical elasticity assessment**

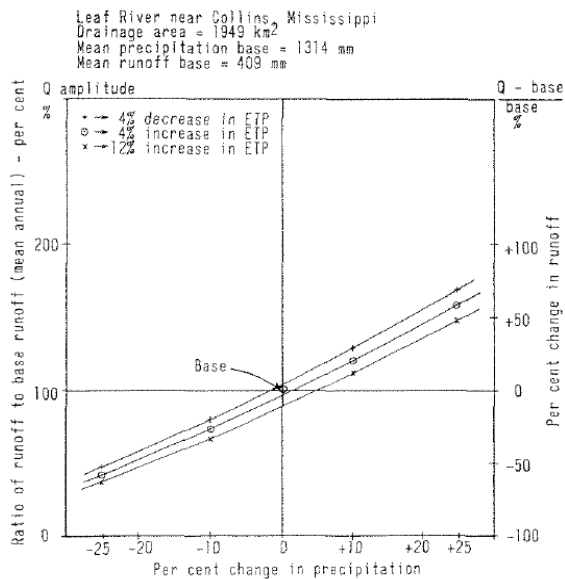
$\Delta Q_i^{(M)} = e_{Q/P}^{(M)} \cdot \Delta P_i^{(M)} + e_{Q/E_P}^{(M)} \cdot \Delta E_{P_i}^{(M)} + \omega_i$		Eq. 13
OLS	$\omega_i \sim N(0, \sigma)$	
GLS	$\begin{cases} \omega_i = \alpha \omega_{i-1} + \delta_i \\ \delta_i \sim N(0, \sigma) \\ \omega_i \sim N(0, \sigma \sqrt{1 - \alpha^2}) \end{cases}$	
$\Delta Q_i^{(M)}$: streamflow anomaly over M years, considered as the explained variable $\Delta X_i^{(M)}$: rainfall or potential evaporation anomaly for the same sub-period, considered as the explanatory variable $e_{Q/X}^{(M)}$: streamflow elasticity (equal to the regression slope) ω_i : regression residual α : parameter of the first-order autoregressive process (AR1) δ_i : innovation of the autoregressive process σ : standard deviation M : number of years over which the long-term streamflow, precipitation and evaporation average is computed		

514

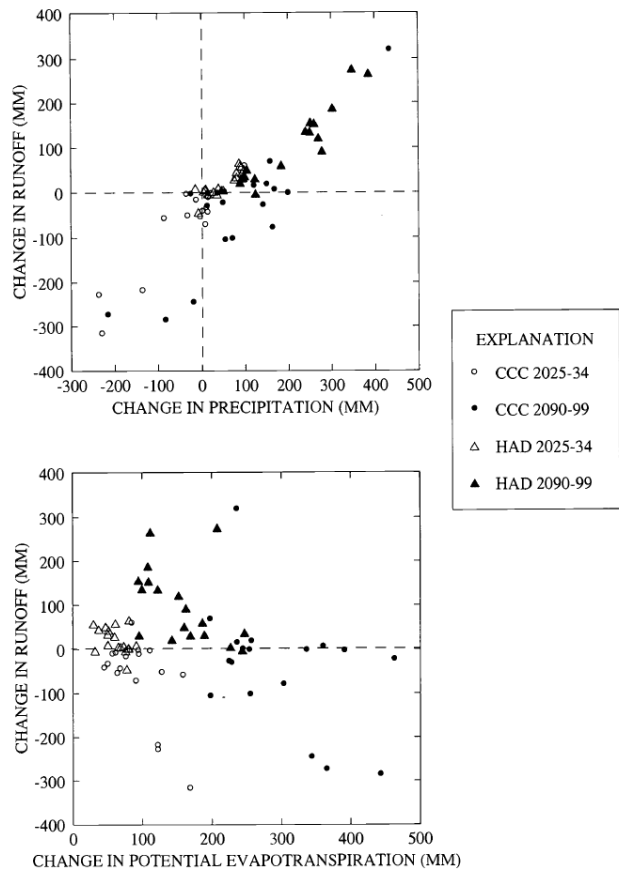


515
516 **Figure 1. Location of the 519 French catchments analyzed in this study**

517
518



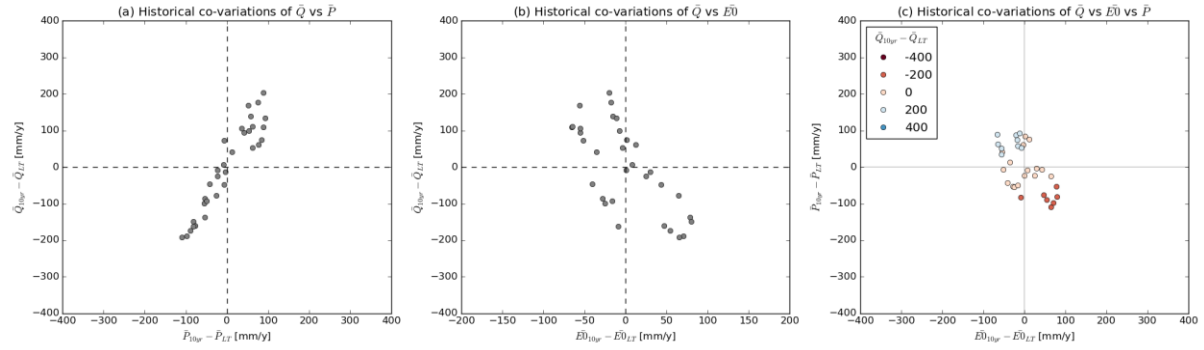
521 **Figure 2. Yield change graph proposed by Nemec and Schaake (1982) to illustrate the**
522 **hydrological elasticity analysis**



524

525 **Figure 3. Elasticity graphs proposed by Wolock and McCabe (1999)**

526



527

528 **Figure 4. Streamflow elasticity graphs for an empirical (data-based) assessment for the Brèze
529 catchment at Meyrueis (code: O3165010): (a) ΔQ vs ΔP , (b) ΔQ vs ΔE_P , (c) ΔQ (color-coded) vs
530 ΔP and ΔE_P**

531

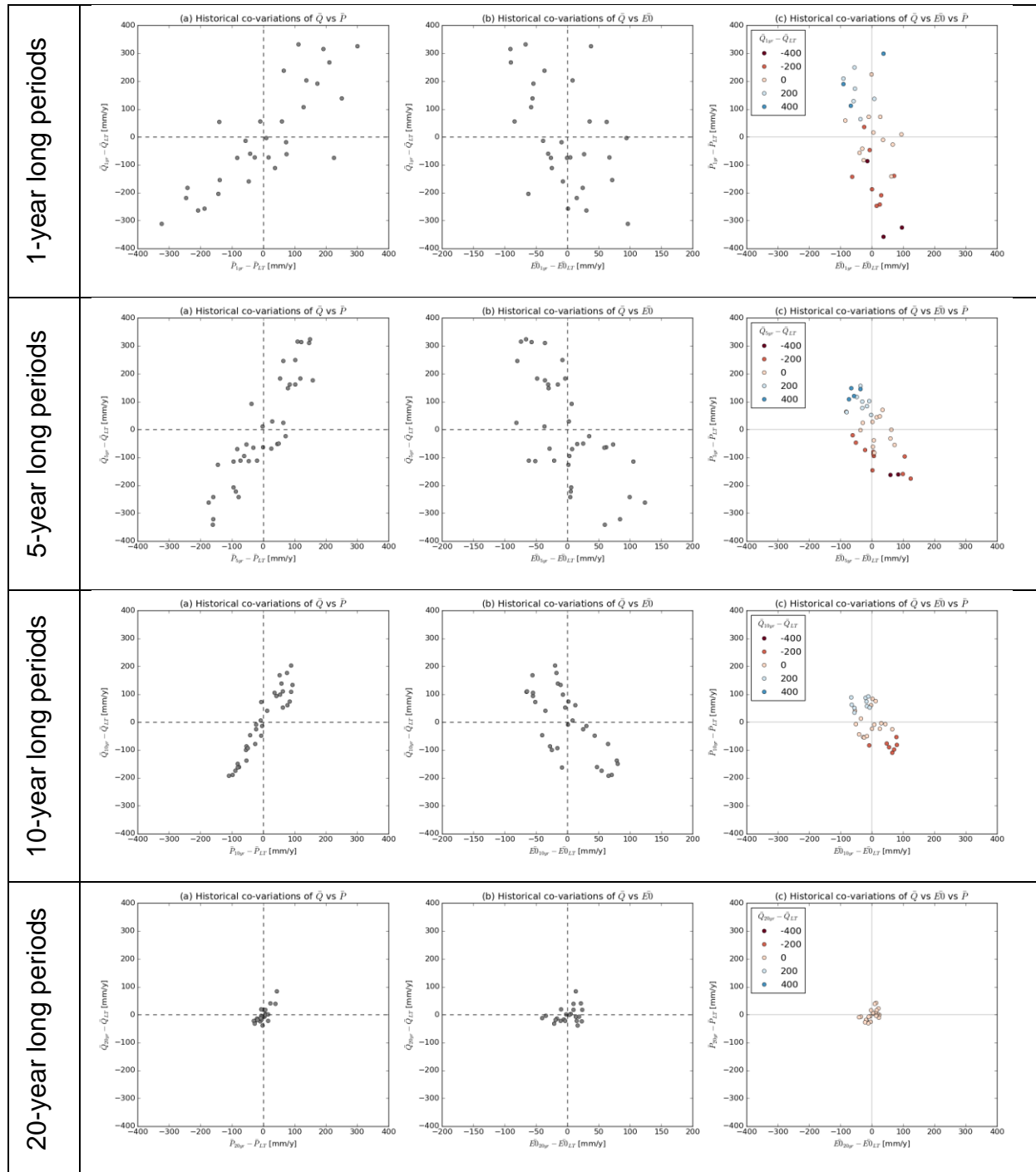
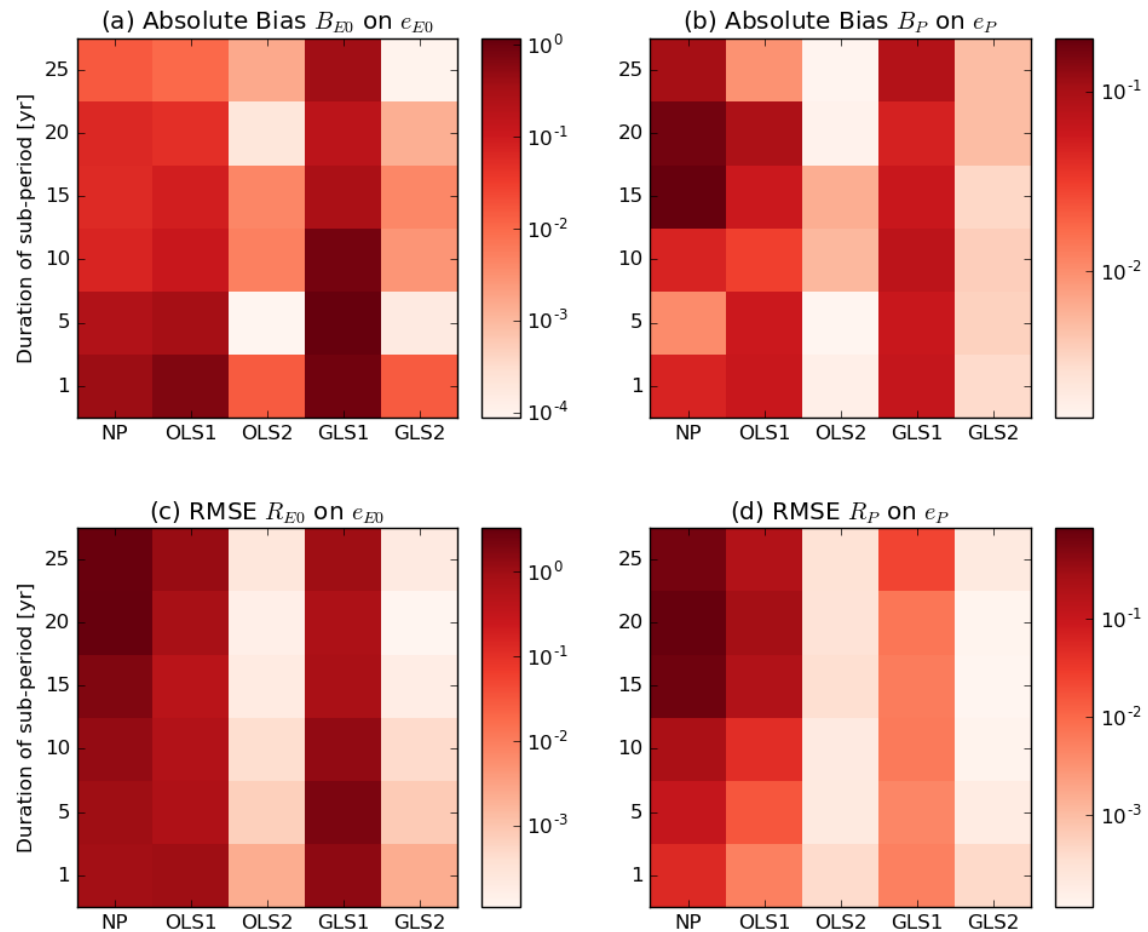


Figure 5. Impact of period length on the streamflow elasticity graphs for an empirical (data-based) assessment. The graphs present from left to right ΔQ vs ΔP , ΔQ vs ΔE_p , ΔQ (in colors) vs ΔP and ΔE_p . LT stands for Long Term (entire period).

532
533
534
535

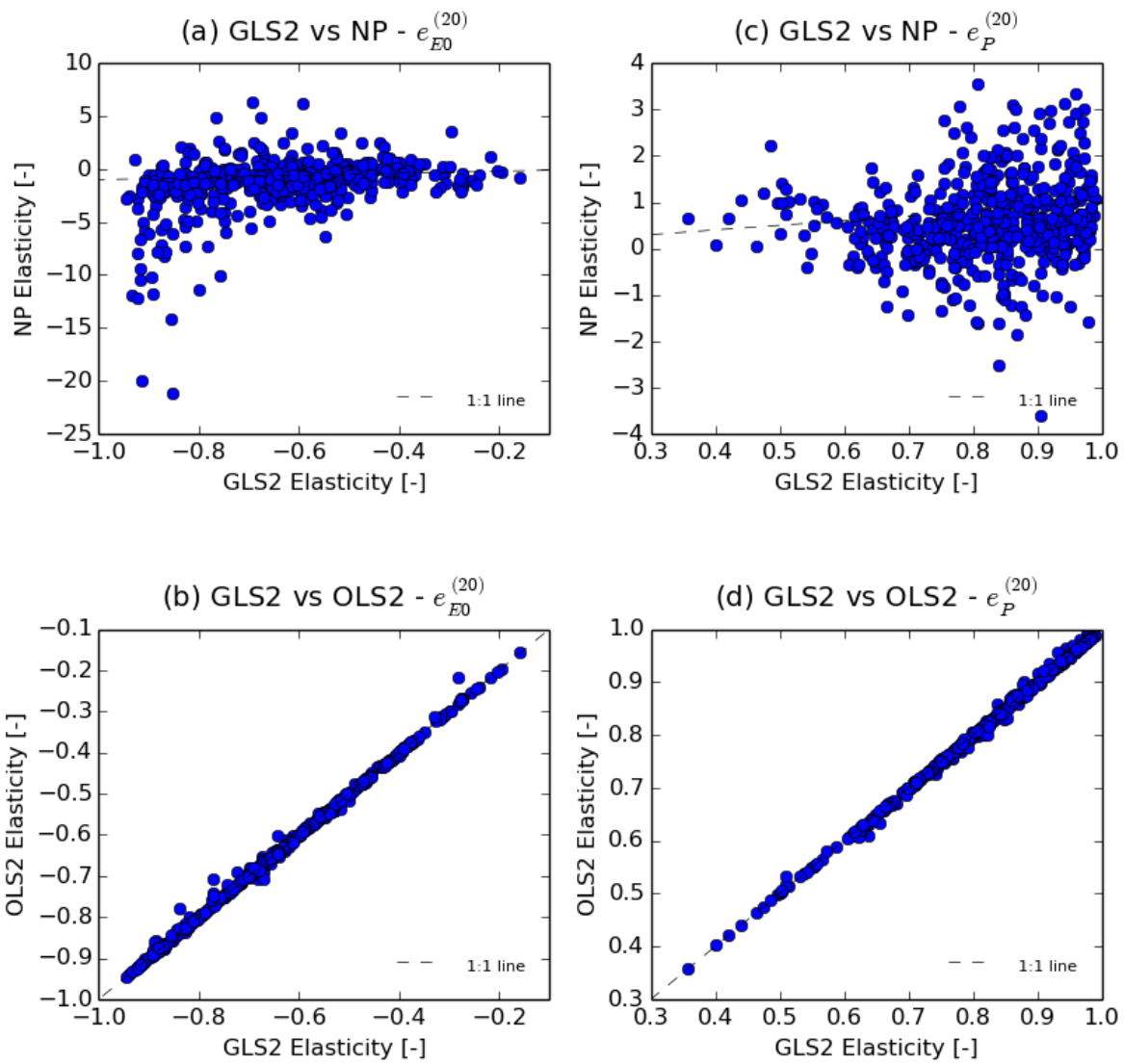
536



537

538 **Figure 6: Performance of the five models proposed to compute empirical elasticity, tested on**
539 **synthetic data generated with the Turc-Mezentsev model.**

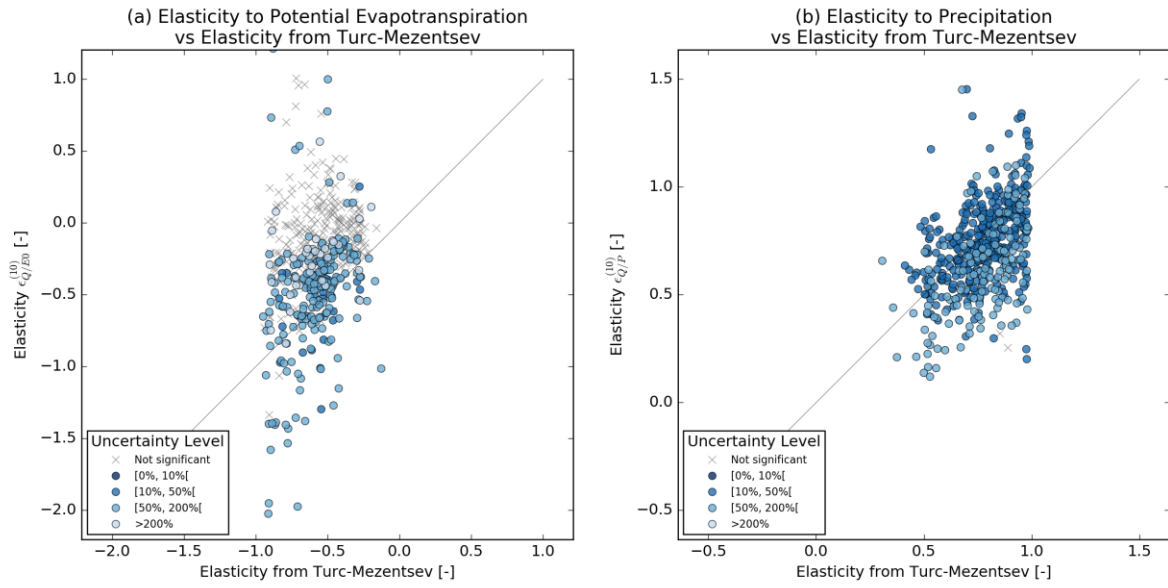
540



541

542 **Figure 7: Comparison of elasticity estimates obtained with the GLS2, OLS2 and NP methods**
 543 **using synthetic flow data and 20-year sub-periods.**

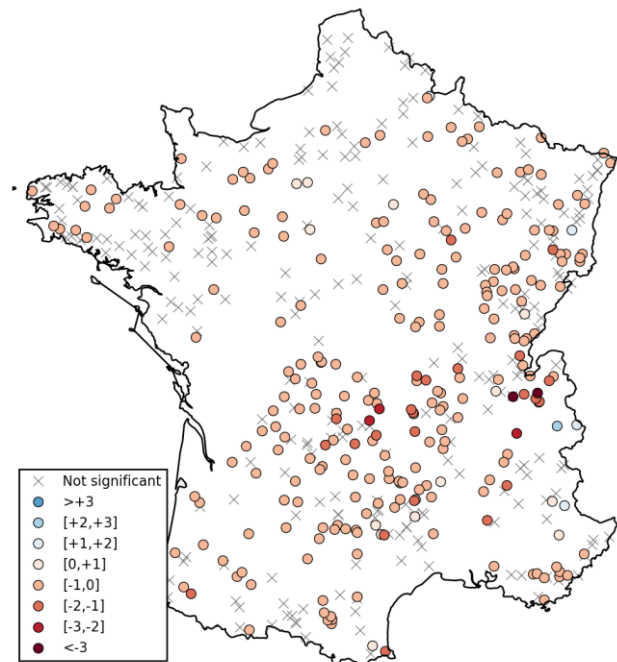
544



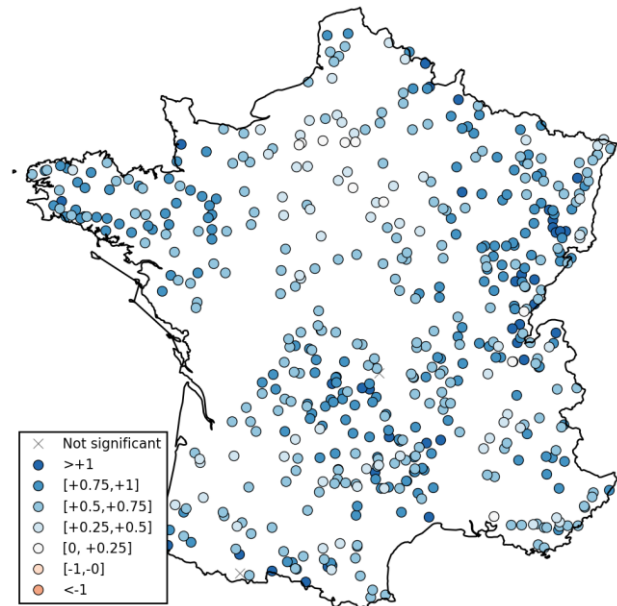
545
546 **Figure 8. Comparison of the data-based and model-based elasticities; streamflow elasticity to**
547 **potential evaporation (a) and precipitation (b).**

548

(a) Elasticity to Potential Evapotranspiration $e_{Q/E0}^{(10)}$



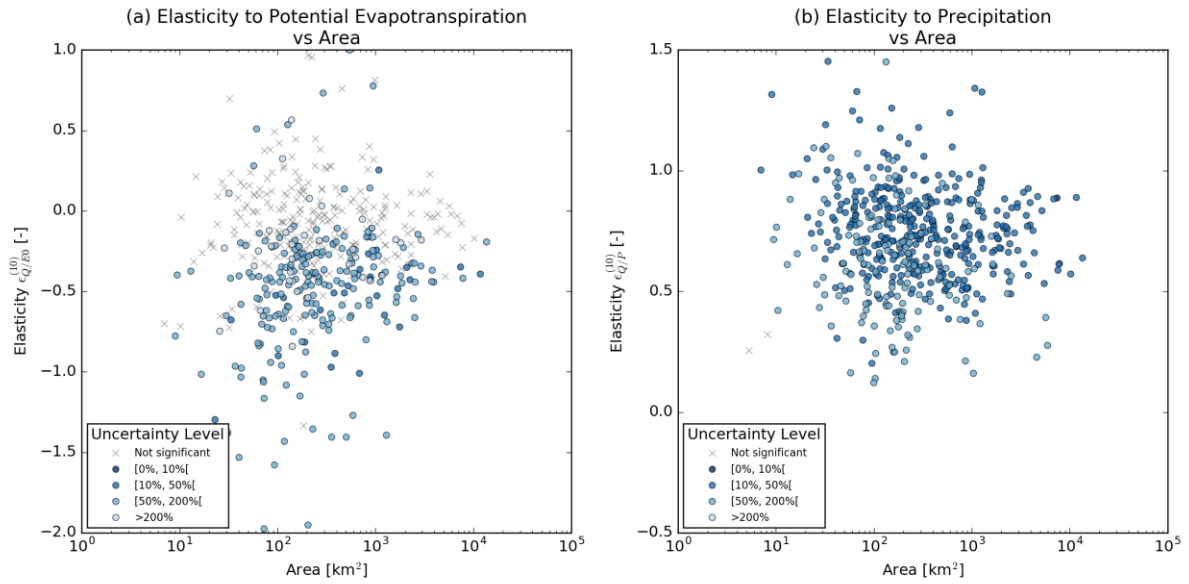
(b) Elasticity to Precipitation $e_{Q/P}^{(10)}$



549

550 **Figure 9.** Regional analysis of (a) streamflow elasticity to precipitation and (b) streamflow
551 elasticity to potential evaporation. Elasticity values were obtained by the GLS2 regression
552 method using 20-year sub-periods. Each dot represents a catchment outlet, the color
553 represents the elasticity value. Those catchments where the linear correlation was found to be
554 nonsignificant are indicated with a cross.

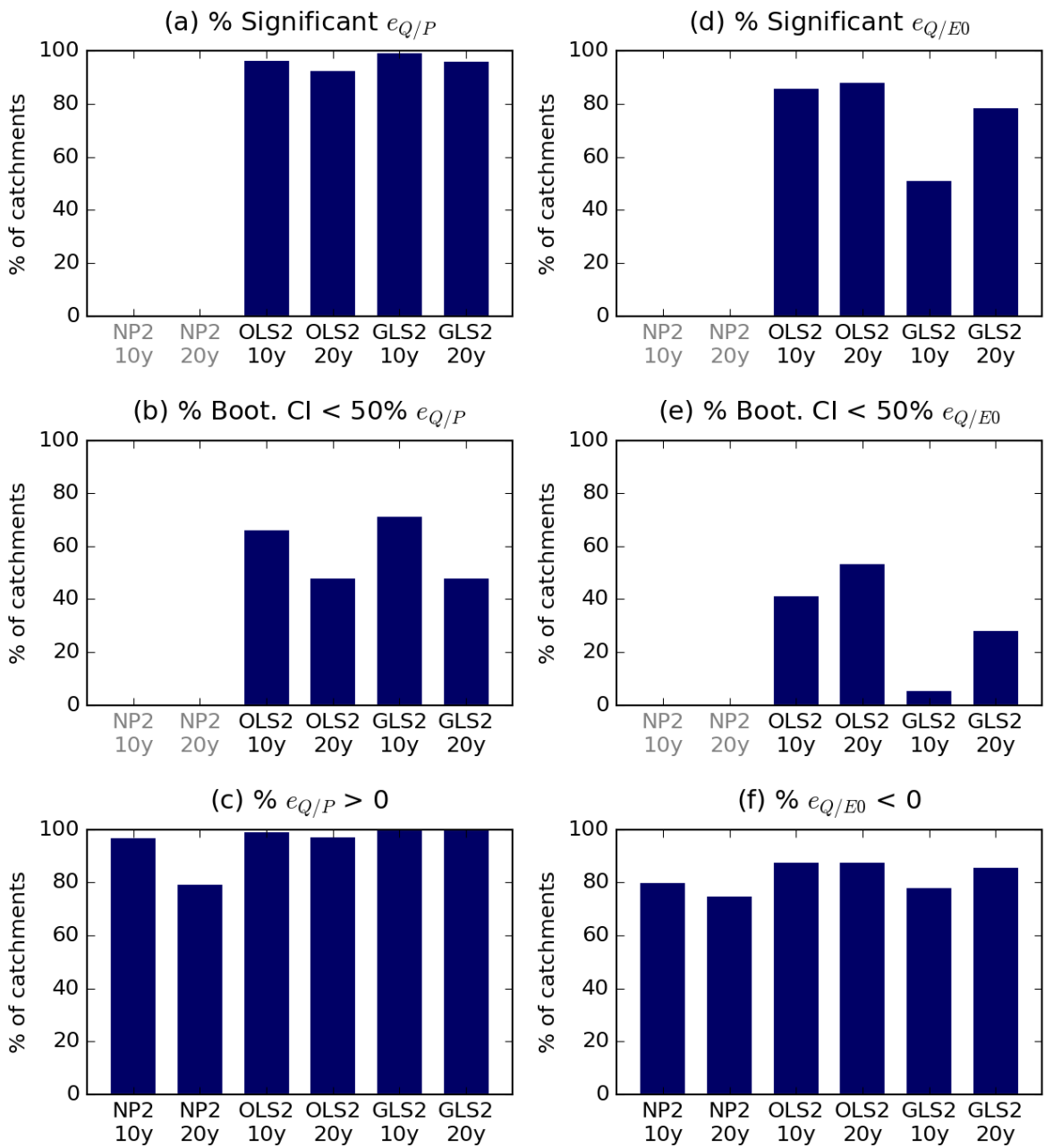
555



556

Figure 10. Elasticity values vs catchment area: (a) streamflow elasticity to potential evaporation and (b) streamflow elasticity to precipitation. Elasticity values were obtained by the GLS2 regression method with 20-year sub-periods.

557



558
559
560
561

Figure 11. Proportion of catchments having a positive outcome for (a) the Shapiro-Wilks normality test and (b) the Durbin-Watson test on autocorrelation of innovations